Chapter

# Flexible Thermoelectric Films and Devices

*Xiang Li and Yao Lu*

## Abstract

Recently, the market for portable, flexible, and wearable electronics has seen explosive growth, paralleled by the burgeoning Internet of Things (IoTs), which encompasses numerous node sensors. The reliance on traditional batteries to power these electronics and IoT node sensors not only poses environmental concerns but also significantly raises costs. Consequently, the self-powering of electronics and IoT sensors has become a necessity. Flexible thermoelectric generators (f-TEGs), assembled with flexible thermoelectric films (f-TEFs), offer a promising solution by continuously harnessing heat energy (such as body heat and sunlight) to power these devices. Consequently, f-TEFs have garnered increasing attention over the past decade, with remarkable breakthroughs occurring in the last several years. In this chapter, we review the recently reported f-TEFs, which could be categorized into freestanding films and films on flexible substrates. Strategies are proposed to improve the thermoelectric (TE) performance of these films. Additionally, we discuss the recent advancements in f-TEFs and illustrate how they can be integrated into generator designs that capitalize on their mechanical and TE properties. Furthermore, we analyze and delve into the challenges and existing problems in the study of f-TEFs and f-TEGs and provide comprehensive design guidelines pertaining to the TE properties and flexibility of the f-TEFs.

**Keywords:** flexible, thermoelectric, flexible devices, composite film, f-TEs

## 1. Introduction

Wearables and Internet of Things (IoT) markets have witnessed an explosive growth in the last decades [1]. The amount of IoT sensors has already surpassed the human population by multiple folds [2]. Wearable electronics, particularly those inspired by skin, serve as cornerstone components for personalized healthcare in the IoT ecosystem [3, 4]. However, the majority of these devices still rely on batteries with finite lifespans, necessitating frequent charging or replacement [5, 6]. This not only elevates operational costs but also contributes to environmental pollution. Furthermore, the limited lifespan of these batteries hinders their further deployment [7, 8]. Consequently, the development of self-powered flexible electronics and sensors that harness energy from the human body is imperative. Thermoelectric generators (TEGs), capable of converting low-grade

waste heat into electricity, offer a practical and feasible solution [9, 10]. TEGs offer several advantages, including the absence of moving parts or fluids, high reliability, and silence in operation. When a TEG is directly attached to the skin, heat naturally flowing from the human body and the TEG could create a voltage through the Seebeck effect based on the thermal gradient between the environment and skin. Then, the electricity produced could be stored in batteries or supercapacitors for subsequent usage, ensuring continuous running of the device [11, 12].

The efficiency of a thermoelectric (TE) generator depends on the figure of merit (ZT), defined as $ZT = S^2\sigma T/\kappa$, where S is the Seebeck coefficient, σ is the electrical conductivity, κ is the thermal conductivity, and T is the absolute temperature. It is evident that the efficiency increases with a higher ZT value. Therefore, to achieve a high-efficiency TEG, we must first identify TE materials with a high ZT. This is challenging because S, σ, and κ are intricately linked to the carrier concentration (n). S represents the average entropy carried by each charge carrier, which decreases as n increases. For metals or semiconductors, S can be calculated by the following formula:

$$S = \frac{8\pi^2 k_B^2}{3eh^2} m^* T \left(\frac{\pi}{3n}\right)^{\frac{2}{3}} \quad (1)$$

Here, $m^*$ denotes the effective mass of the carriers, while $k_B$ represents the Boltzmann constant and h represents Planck constant. σ is proportionate to the n and carrier mobility (μ), given by the relationship $\sigma = ne\mu$. κ primarily consists of phonon thermal conductivity ($\kappa_L$) and electronic thermal conductivity ($\kappa_e$), where $\kappa_e$ is in proportion to σ based on the Wiedemann-Franz Law ($\kappa_e = L\sigma T$), albeit this relationship does not hold for organic materials. Consequently, decoupling these three variables and achieving a high ZT is exceedingly challenging.

Traditional TE materials are primarily inorganics. Numerous tactics such as nanotechnology [13], energy band engineering [14], and defect engineering [15] have increasingly been employed to enhance their TE performance. Consequently, some inorganics, such as PbTe [16] and SnSe [17], have demonstrated ZT values exceeding 2. However, nearly all inorganic TE materials are rigid and inflexible, making them unsuitable for wearable platforms. Therefore, one of the primary challenges in developing f-TEGs with high efficiency is to identify f-TEFs with excellent TE properties.

Conducting polymers (CPs), such as poly(3,4-ethylenedioxythiophene) (PEDOT) [18–20], polyaniline (PANI) [21, 22], and polypyrrole (PPy) [23, 24], exhibit remarkable bendability, lightweight, and low κ [25, 26]. Consequently, in the past decade, research on flexible TE materials has predominantly focused on CPs and their composites with inorganic TE materials. This focus aims to leverage the low thermal conductivity and excellent flexibility of CPs, while also benefiting from the high PF of inorganics [27, 28].

Recently, insulating polymers (IPs) typically including polyvinylidene fluoride (PVDF) [29], epoxy resin [30], polylactic acid (PLA) [31, 32], and polyvinyl pyrrolidone (PVP) [33] have been selected as matrices for f-TEFs. Additionally, carbon materials, such as fullerene [34], carbon nanotube (CNT) [35–37], and graphene [38], as well as carbon material-based composites [39–42], have garnered significant attention due to their impressive σ, flexibility, and light-weight. Nevertheless, inorganic alloys are most widely researched because of the superior TE performance. Consequently, inorganics-based f-TEGs have garnered more attention, and recently, notable advancements have been achieved (see **Figure 1**).

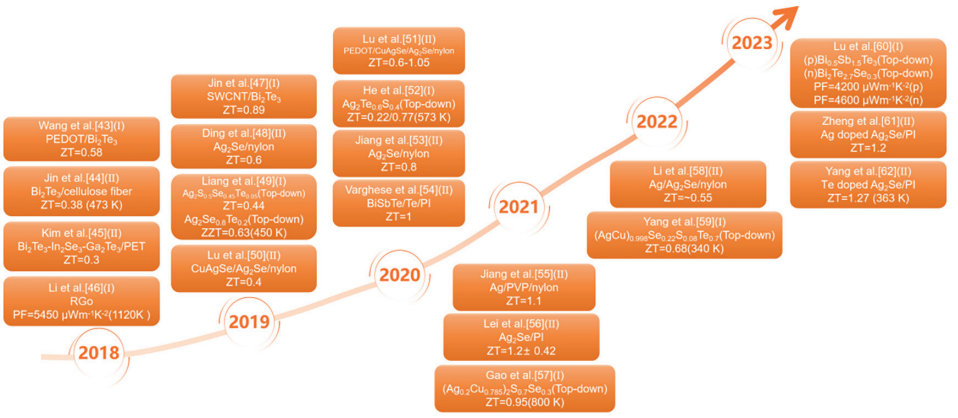


**Figure 1.**
*Some representative works about f-TEFs in the last decades [43–62]. "I" denotes freestanding f-TEF; "II" denotes f-TEF on substrate.*

The traditional method for preparing films involves utilizing rigid substrates, as these facilitate the achievement of films with superior TE performance compared to films grown on flexible substrates. However, the unbendability of these substrates inherently limits the flexibility of the resultant films. Consequently, researchers have increasingly focused on developing films on flexible substrates.

Another significant challenge in the development of f-TEGs lies in their rational design, which includes optimizing the size of f-TEGs' legs, ensuring adequate contacts, thermal interfaces, and packaging methods. This aspect of research relatively lagging behind compared to the study of f-TEFs [63, 64]. Currently, the development of f-TEGs is still at the proof-of-principle demonstration stage [65]. Based on their operation mode, f-TEGs are categorized into two types. The first type is prepared by connecting p- and n-type inorganic TE bricks electrically over a flexible substrate with patterned electrical contacts. Here, the temperature difference across the bricks is perpendicular to the substrate [66–68]. The second type is created by either directly fabricating TE legs onto a flexible substrate or by cutting strips from films, assembling them, and adhering them onto the substrate. In both cases, the TE legs harness electricity from the thermal gradient that exists in the in-plane direction of the strips [69–74]. The first form of f-TEGs always lack sufficient flexibility. This chapter will focus solely on the latter form, which is lightweight and highly flexible.

The approximate voltage ($V_{voltage}$) produced by a TEG can be expressed as:

$$V_{voltage} = N\left(S_p - S_n\right)\Delta T \tag{2}$$

where $S_p$ and $S_n$ represent the Seebeck coefficients of the p-type and n-type semiconductors, respectively, and *N* denotes the number of p-n thermocouples [75–79].

$$P = UI = \frac{U^2}{R_{ex} + R_{in}} \tag{3}$$

When the external load resistance ($R_{ex}$) is equal to the internal resistance of the device ($R_{in}$), the output power reaches its peak value [80, 81]. The maximum power

density ($P_{density}$) is calculated by dividing the generated power by both the cross-sectional area (A) and the total number of legs ($N_l$), as outlined in the following equation:

$$P_{density} = \frac{P_{max}}{N_l \cdot A} = \frac{(N_l \cdot S \cdot \Delta T)^2}{N_l \cdot A} \cdot \frac{\sigma \cdot w \cdot t}{4 \cdot N_l} = \frac{S^2 \cdot \sigma}{4l} \cdot \Delta T^2 \quad (4)$$

where w, d, and l, respectively, denote the width, thickness, and length of the legs. The varying temperature differences and lengths employed in different applications necessitate the introduction of normalized power density, $P_{density} \bullet l/\Delta T^2$, which facilitates comparisons of the devices' output performance [82, 83].

In this chapter, we initiate with a systematic review of f-TEFs, which are categorized into two types: (i) free-standing f-TEFs and (ii) f-TEFs on substrates (see **Figure 2**). Considering that the output density of existing devices fails to meet practical power supply requirements, this chapter attempts to address the issue from two perspectives: materials and device design, aiming to pave a route for future researchers. To be more specific, this chapter is structured around two primary parts. Firstly, we comprehensively examine free-standing f-TEFs by analyzing various material systems. Secondly, we classify f-TEFs on substrates based

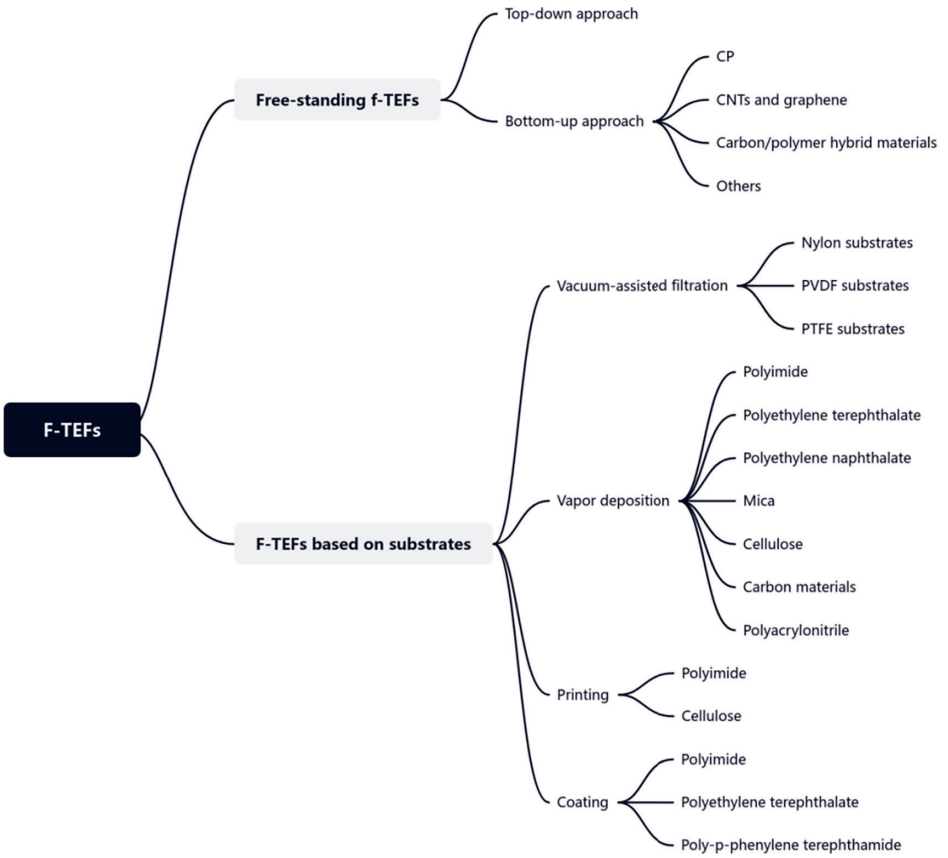


**Figure 2.**
*The mind map of this chapter.*

on the diverse flexible substrates utilized. Lastly, we highlight the main challenges in the study of f-TEFs and propose feasible solutions.

## 2. Freestanding film

Freestanding films could be prepared using top-down or bottom-up approaches. The top-down method involves creating large-scale templates and subsequently reducing their lateral dimensions to the nanoscale. This method has the advantage of being able to produce high-quality, high-performance materials, but it is also limited by the availability of material systems and its expensive, energy-intensive preparation process. Bottom-up method involves constructing multifunctional nano-sized materials through the self-assembly of atoms or molecules. This technique relies on the chemical reaction of precursors under specific reaction conditions, offering advantages such as low cost, simplicity of operation, and suitability for industrialization. However, it also has drawbacks, including poor controllability, the need for post-treatment, and low product quality due to poor crystallinity.

### 2.1 Top-down approach

The "top-down" approach to obtain inorganic f-TEFs entails the fabrication of bulks through traditional melting or annealing techniques, subsequently slicing them into thinner sections. Some progress have been made in this field (see **Figure 3**) [78].

In 2018, zone melting process was adopted by Shi et al. [79] to synthesize a range of Te/Se-doped $Ag_2S$-based TE materials, followed by spark plasma sintering. These bulk materials were then sliced into thin sections, which exhibited favorable mechanical properties. Notably, the ZT value reached 0.44 for $Ag_2S_{0.5}Se_{0.45}Te_{0.05}$ at RT and 0.63 for $Ag_2S_{0.8}Te_{0.2}$ at 450 K. Later on, Lu et al. [60] utilized the similar process to prepare p- and n-type $Bi_2Te_3$-based flexible films, achieving elastic bending (with only a 9% decrease in σ after 1000 bending tests at a 4 mm bending radius) due to the staggered-layered structure, while minimizing the degradation of carrier transport along the temperature difference, reaching high PF values of 4200 (p-type) and

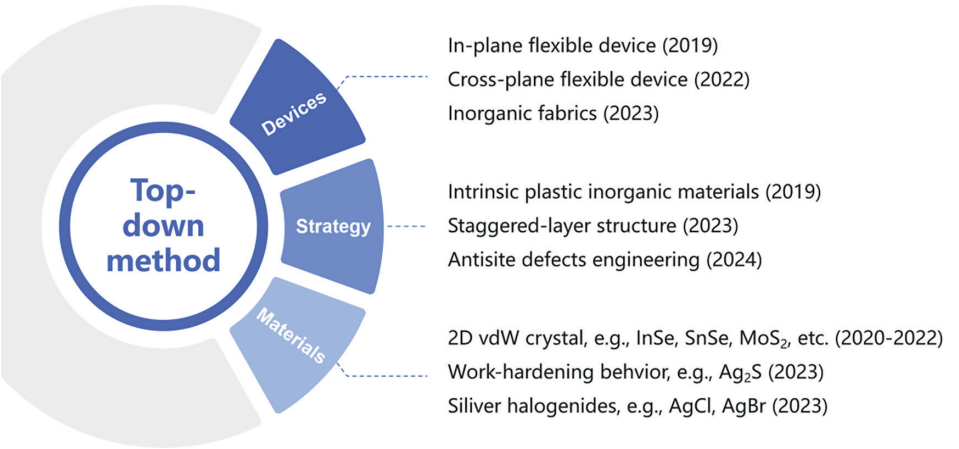


**Figure 3.**
*Brief summary of plastic inorganic TE materials.*

4600 (n-type) $\mu W/mK^2$ at RT, respectively. Very recently, Deng et al. [80] discovered that, in brittle bismuth telluride-based materials, the induction of high-density and diversified microstructures through modulation of antisite defects achieved a transformation from brittleness to plasticity. This enhancement elevated the ZT at RT to approximately 1.0, which is comparable to that of traditional brittle thermoelectric materials.

Despite the advancements, significant challenges persist within this emerging field, primarily encompassing an inadequate comprehensive grasp of the deformation mechanism, hurdles in synergistically adjusting both TE performance and deformability, as well as a scarcity of technological breakthroughs in both processing this novel class of TE materials and their seamless integration into devices.

## 2.2 Bottom-up approach

The bottom-up methodology entails constructing structures one atom or one molecule at a time, utilizing covalent or supramolecular interactions, analogous to the process of building a house one brick after another. This method can be realized through several approaches:

1. Initially, a precursor solution is either drop-cast or spin-coated onto a substrate, followed by peeling the resulting film. The contact angle determines the ease of preparing the film, i.e., the greater the angle of the solution droplet on the substrate, the more likely it is to detach the formed film [81].

2. Using the pressure difference between the two ends of the filter membrane via vacuum-assisted filtration, solid particles in the liquid are retained on the membrane and self-assembled to form a thin film, which is subsequently peeled off [82].

3. A self-supporting CP film or carbon-based substrate, upon which the TE inorganic is deposited through deposition process, such as electrodeposition [83].

4. Bacterial action in a petri dish could facilitate the in situ formation of composite films with bacteria cellulose as a matrix [84].

5. Interfacial polymerization method could be utilized to prepare a freestanding film at the liquid-liquid or liquid-air interface.

6. After mixing various materials using the centrifugal force generated by high-speed centrifugation, a film could be formed on the substrate material and then peeled off [85].

   Below, we provide a detailed review of the progress of related self-supporting films, categorized by material systems.

### *2.2.1 CP*

Since the late 1970s, when doped polyacetylene was first discovered, CPs have garnered significant interest as a crucial polymer. Typically, CPs behave as semiconductors and exhibit electronic conductivity once doped with appropriate dopant

materials and their high σ combining with excellent plasticity makes it attractive as TE matrices. PEDOT is one of the most extensively studied CPs in terms of excellent σ and stability. But the insolubility pose challenges for processing. To date, the mainstream method is to utilize poly(styrenesulfonate) (PSS) to decorate PEDOT. To mitigate the insulating effect of PSS, pure PEDOT film could be prepared as template [86, 87]. Apart from PSS, other dopants, like tosylate (Tos), are also used to improve the water-solubility of PEDOT [18, 41, 88]. For instance, Bubnova et al. [89] employed Tos to dope PEDOT (not in the form of a flexible film) to adjust its oxidation level, achieving a room-temperature ZT value of 0.25 with a high S of 220 μV $K^{-1}$. Subsequently, significant research has been conducted on post-treatment and doping of PEDOT. Post-treatment is often utilized to adjust the conformation and oxidation state of PEDOT, typically involving treated by polar solvents such as $H_2SO_4$, ethylene glycol, or through heat treatment. The other route designed by Fan et al. [90] to significantly improve the S involved creating a heterogeneous structure inside PEDOT:PSS via introducing ionic liquids (not a flexible film), which caused ion accumulation that scattered charge carriers with low energy, thereby significantly enhancing the S while σ almost remaining constant, leading to a PF up to 754 μW $m^{-1}$ $K^{-2}$. **Figure 4** depicts the comparison of σ and S in PEDOT:PSS films doped by various agents.

### *2.2.2 CNTs and graphene*

Up to now, numerous studies have focused on preparing CNT bucky papers with a thickness commonly between 50 to 200 μm, subsequently applying post-treatment

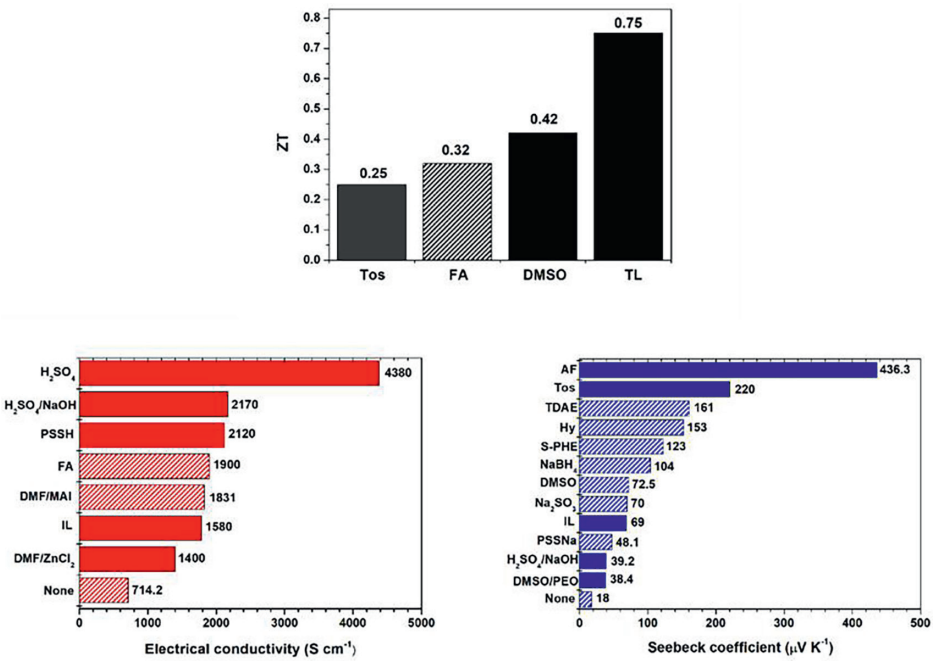


**Figure 4.**
*Comparison of σ and S in PEDOT:PSS with different treatments, where the column filled with slashes represents the flexible film and solid column represents inflexible film. These data have been sourced from refs [91–98]. Image reproduced with permission from Ref. [72] published by Elsevier.*

to enhance their inherently low TE properties. For example, An et al. [99] subjected spun CNT bucky paper to post-treatment combining heat treatment and doping with benzyl viologen, achieving a PF of approximately 3103 μW $m^{-1}$ $K^{-2}$ at RT. Interestingly, polyetherimide was found to transfer the CNT from p-type to n-type [100]. Meanwhile, the TE properties of graphene could be also improved by post-processing techniques. For instance, Li et al. [46] reduced graphene oxide film at high temperatures, resulting in a film that exhibited a peak PF of 5450 μW $m^{-1}$ $K^{-2}$ at 1120 K and remained to have excellent thermal stability, making it suitable for applications at extremely high temperatures.

### *2.2.3 Carbon/polymer hybrid materials*

Due to their extensive π-conjugated structure and substantial specific surface areas, carbon nanoparticles could significantly enhance effective interfacial interactions with polymers. And, the high κ of these nanoparticles can be modulated through encapsulation or connection with polymers, and μ could also be substantially elevated. Researchers have endeavored to develop carbon nanoparticles/polymer f-TEFs [36, 38, 40, 42, 101, 102]. For example, Wu et al. [103] drop-casted SWCNTs dispersion onto the as-prepared PANI film, which facilitated to transfer the CP from a coiled state to a tensile state to form a highly ordered PANI interface, and thereby a high σ ~4000 S $cm^{-1}$ was achieved.

### *2.2.4 Others*

Given the intrinsic low S of polymers and carbon materials, incorporating inorganic TE elements as fillers into these matrices has increasingly become a prevalent approach to fabricate freestanding f-TEFs. The rationale behind this approach includes the following: (i) the relative high PF in inorganics, (ii) an improvement in the S through the energy-filtering effect, and (iii) a reduction in κ resulted from phonon scattering upon the interfaces.

However, achieving a robust combination between organic and inorganic materials presents a significant challenge due to their vastly different chemical properties. Therefore, the preparation of organic-inorganic hybrid f-TEFs with high TE performance is a critical concern.

In situ composite approach, involving the direct synthesis of reinforcing phases within the matrix, has been proved to be an effective method. For example, Wang et al. [43] employed polystyrene nanospheres as template to in situ crystallize $Bi_2Te_3$ nanoarrays, followed by deposited PEDOT upon the arrays to create a hybrid f-TEFs. The energy filtering effect and the strong acoustic mismatch between PEDOT and $Bi_2Te_3$ was considered to improve the ZT value to 0.58 at RT. Similarly, Jin et al. [47] utilized CNT as a template to deposited Bi–Te atoms, and the in situ crystalization on CNT contributes to the high orientation and low angle grain boundaries of $Bi_2Te_3$ nanocrystals, resulting in an excellent ZT value of ~0.89 at RT. Recently, Xu et al. [104] employed a wet-chemical method to create a flexible PVDF/$Ta_4SiTe_4$ film. The dimensionality/morphology matching strategy was proposed to guide the $Ta_4SiTe_4$ whiskers seamlessly interfaced with the polymer, resulting in a PF of 576 μW $m^{-1}$ $K^{-2}$ at RT.

Two-dimensional materials like $Bi_2Te_3$ and transition metal dichalcogenides have attracted attention for their unique in-plane electronic properties and large surface areas. Weak van der Waals interactions enable easy exfoliation into nanosheets (NSs) for composite processing. For instance, Du et al. [105] used lithium-ion intercalation to exfoliate

$Bi_2Te_3$-based alloys, mixing them with PEDOT:PSS to form freestanding f-TEFs. Similar approaches were applied to SnSe-based/PANI films [106, 107] and $MoS_2$/CNTs films [108]. Apart from physical (e.g., mechanical or liquid-phase exfoliation using solvents with matching surface tension [109, 110]), chemical exfoliation approach is also effective. For example, Dun et al. [111] intercalated Cu into $Bi_2Se_3$ nanoplatelets, dispersing them in PVDF to create a freestanding f-TEF with a ZT of 0.1 near RT.

Intercalation is also effective for tuning carrier transport. Wan et al. [112] intercalated organic molecules into $TiS_2$ layers, selectively removing some during heat treatment to reduce n, enhancing PF to 904 μW $m^{-1}$ $K^{-2}$ at RT. Organic layers in the interspace lowered κ, achieving an ZT of ~0.33 at 413 K. Overall, reducing polymer content while maintaining flexibility enhances TE performance.

## 3. Flexible film based on substrate

### 3.1 Vacuum-assisted filtration

Vacuum filtration is a commonly used method for preparing thin films, featuring simple operation and low cost. Its main principle involves depositing material molecules onto the substrate surface through vacuum adsorption technology, thereby forming a nanoscale thin film. This method boasts advantages such as producing thin films with high purity, high density, high compactness, and strong adhesion. Thanks to their high chemical stability, nylon-based, PVDF-based, and PTFE-based filter membranes are widely used in thin film preparation processes. In the following sections, we will review the relevant works in detail, one by one.

#### *3.1.1 Nylon membrane*

Cai's group [113] was the first to utilize nylon membranes as substrates for preparing TE films using vacuum-assisted filtration. They successfully integrated SWCNTs as fillers into a highly conductive PEDOT:PSS to create p-type TE films with an optimal PF of 83.9 μW $m^{-1}$ $K^{-2}$. Further, they [114] introduced Te nanorods with a high S [115] into this system and significantly improved the PF to 104 μW $m^{-1}$ $K^{-2}$ at RT. Similarly, PEDOT/SWCNT f-TEFs were also reported by Fan et al. [116], with a PF doubled compared with the previous work [114].

It is well-known that inorganic TE materials exhibit superior TE performance. Therefore, it is desirable to combine the high TE properties of inorganic materials with the excellent flexibility of organic substrates. Cai's group [48] developed a novel method to achieve this goal, that is, firstly preparing $Ag_2Se$ NWs and then utilizing vacuum filtration to form the film on a nylon membrane combining with post hot-pressing treatment at 573 K and 1 MPa for 30 min. And finally, they obtained a porous $Ag_2Se$ film on nylon with a PF of 987.4 μW $m^{-1}$ $K^{-2}$ and a ZT of approximately 0.6 at RT, accompanied with excellent flexiblity (**Figure 5a-d**). To enhance the PF of the $Ag_2Se$ film, they [53] tried to raise the synthesis temperature or incorporate IPs, like PVP [55], into the system, and the resulted PF was successfully increased by an order of magnitude, up to ~1910 μW $m^{-1}$ $K^{-2}$ at 300 K (**Figure 5e-h**).

On the other hand, Lu et al. [51] successfully incorporated $Cu^{2+}$ into the synthesis of $Ag_2Se$ nanowires to improve the TE performance via the energy filtering effect (as illustrated in **Figure 5i**), thereby achieving an impressive PF of approximately 1593 μW$m^{-1}$ $K^{-2}$. Further, Lu et al. [50] introduced PEDOT:PSS in situ during the growth

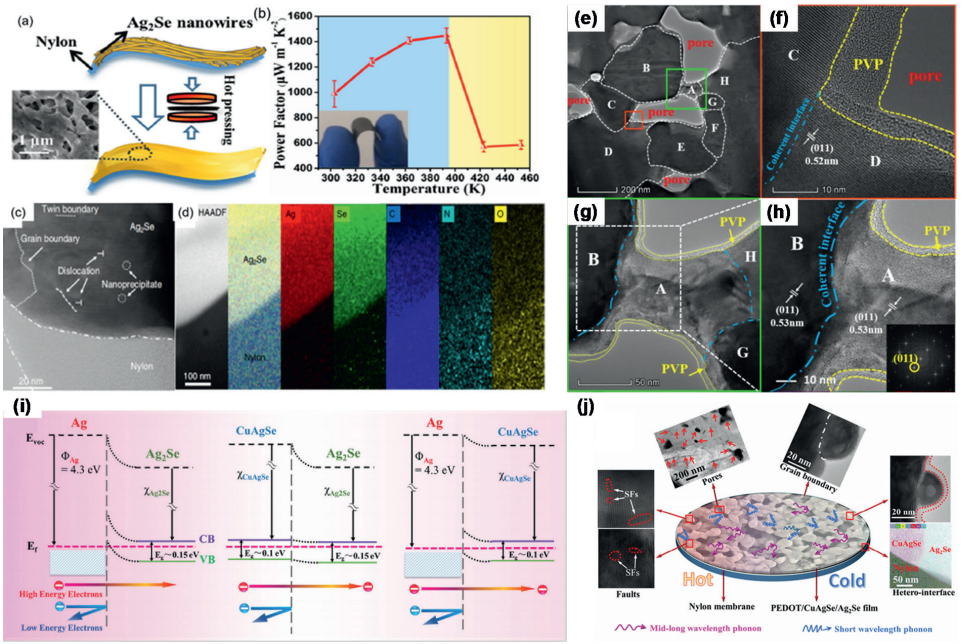


**Figure 5.**
*(a) Schematic of $Ag_2Se$/nylon film. (b) PF vs. temperature plot for the film. (c) HRSTEM image showing seamless $Ag_2Se$-nylon integration. (d) HAADF image of $Ag_2Se$-nylon heterointerface, EDS mapping, and elemental images for Ag, Se, C, N, and O (Ref. [48], Springer Nature). (e) TEM cross-sectional image of the film showing pores and grains (A-G). (f) Enlarged view of (e) red square. (g) Zoomed view of (e) green square with PVP-coated $Ag_2Se$ grains. (h) HRTEM of (g) white square (Ref. [55], Elsevier). (i) Band diagram for Ag/$Ag_2Se$, CuAgSe/$Ag_2Se$, and Ag/CuAgSe interfaces (Ref. [50], RSC). (j) Diagram of phonon scattering in PEDOT/CuAgSe/Ag2Se film (Ref. [51], Elsevier).*

of $Ag_2Se$/CuAgSe Nws to reduce the thermal conductivity. And the composite film exhibited a remarkable PF of approximately 1603 W $m^{-1}$ $K^{-2}$, corresponding to a ZT value within the range of 0.6 to 1.05 at 300 K due to the hierarchical microstructure defects inside (as illustrated in **Figure 5j**). Generally, the methodology outlined above could also be adapted to other TE components, like Ag/$Ag_2Te$/PVP films [33] and PEDOT:PSS/$Cu_2Se$ films [66].

Concurrent with above work [48], Zeng et al. [117] also reported the fabrication of an $Ag_2Te$ film on a nylon filter membrane through vacuum filtration, followed with mechanical-thermal welding. This hybrid film exhibited an impressive PF of approximately 315.1 μW $m^{-1}$ $K^{-2}$ around 400 K. Leveraging this film, a TE sensor was developed, boasting a swift response time of only 1.05 seconds—faster than many similar documented sensors [118–121].

The aforementioned studies underscore the potential of nylon membranes as exceptional substrates for hosting inorganic TE films or inorganic/polymer hybrid films. By integrating vacuum filtration with subsequent heat treatment, these films can achieve superior TE performance while maintaining exceptional flexibility.

### *3.1.2 PVDF membrane*

PVDF filter membrane possesses high chemical stability, excellent mechanical strength, and heat resistance. Thanks to the porous structure of PVDF enabling

the removal of excess PSS during the filtration process, a range of composite films, based on PEDOT:PSS, has been successfully fabricated onto PVDF substrates. For instance, Jiang et al. [122] employed a physical mixing method to create a PEDOT:PSS/SiC NWs composite film, which exhibited an enhanced S of 20.9 μV $K^{-1}$ due to an energy-filtering effect. Notably, after treatment with $H_2SO_4$ to eliminate non-conductive PSS, σ skyrocketed to 3113 S $cm^{-1}$, resulting in an optimized PF of 128.3 μW $m^{-1}$ $K^{-2}$ at RT. See et al. [123] synthesized a PEDOT:PSS-coated Te nanorod composite film on a quartz substrate. Also, Novak et al. [124] prepared graphene on a PVDF membrane and the film showed a PF of 673 μW $m^{-1}$ $K^{-2}$ (RT).

In addition to these two filter membranes, PTFE membranes can serve as effective substrates. While PTFE membranes may not offer the same level of flexibility of these two membranes, their temperature tolerance, which is at least 320°C, surpasses that of other filter papers. Therefore, for applications requiring higher temperature treatment (>400°C), such as with $Bi_2Te_3$, PTFE membranes would be a more suitable choice.

### 3.2 Vapor deposition

Vapor deposition is a well-established technique for depositing films onto substrates, encompassing both chemical and physical vapor deposition. This process typically necessitates high temperatures, making it imperative that the substrate maintains stability under such conditions.

#### *3.2.1 Polyimide (PI)*

Zhu et al. [125] deposited $Bi_2Te_3$-based alloy films on PI substrates via magnetron sputtering, followed by annealing at 573 K, achieving PFs of 769 and 400 μW $m^{-1}$ $K^{-2}$ for p- and n-type films, respectively. RF magnetron sputtering was later used to deposit Te/$Bi_2Te_3$ on PI, with annealing at 673 K enhancing crystallinity and raising PF to 1145 μW $m^{-1}$ $K^{-2}$ [126]. Nuthongkum et al. [127] optimized PF to 1200 μW $m^{-1}$ $K^{-2}$ at 195°C by adjusting sputtering pressure. Further increases in pressure yielded PFs of ~2170 μW $m^{-1}$ $K^{-2}$ for $Bi_2Te_3$ and 1750 μW $m^{-1}$ $K^{-2}$ for $Sb_2Te_3$ [128]. Improvements were attributed to reduced grain size, diminished gaps, and preferential orientation.

Similarly, Shen et al. [129] found enhanced crystallization and reduced porosity at 4 Pa, achieving a PF of ~518 μW $m^{-1}$ $K^{-2}$ for $Sb_2Te_3$. Khumtong et al. [130] reported that lower pressure improved grain size and crystallinity, while higher pressure enhanced film formation, achieving a PF of 1060 μW $m^{-1}$ $K^{-2}$ at 1 Pa.

Jitthamapirom et al. [131] compared DC and RF sputtering, with DC achieving a PF of ~3500 μW $m^{-1}$ $K^{-2}$ at 558 K, significantly outperforming RF sputtering. Additional strategies, such as preventing element re-evaporation [132], doping [133, 134], and substrate selection [135], further enhanced TE performance.

Beyond Bi-Te alloys, Zn-Sb films have gained attention due to their non-toxic composition. Fan's group [136, 137] incorporated Ti into Zn-Sb alloys using multi-step sputtering, reducing defects and achieving a PF of ~3590 μW $m^{-1}$ $K^{-2}$ at 250°C. Toko et al. [138] applied this technique to Ge-based films, achieving a PF of 190 μW $m^{-1}$ $K^{-2}$. Transparent TE films with ZT ~0.29 were also developed using CuI or Ga-doped ZnO on PI substrates [139].

### 3.2.2 Polyethylene terephthalate (PET)

PET stands as another exceptional polymer substrate for the fabrication of fully transparent films. Yang and his team [140], for instance, employed reactive sputtering at room temperature to deposit γ-CuI films on both PET and glass substrates. The film that deposited on the glass substrate showed a ZT of approximately 0.21 at RT, which surpassed the performance of other transparent materials during that period. Furthermore, it was observed that compressive stress enhanced σ, whereas tensile stress led to a reduction in σ. This phenomenon can be attributed to changes in the compactness of the grains. Notably, a P of 8.2 nW at a thermal gradient of 11 K was generated through a transparent f-TEGs with a single leg.

Additionally, Seo and colleagues [141] designed removable f-TEGs by depositing $Bi_2Te_3$ and Cu electrodes directly onto a PET substrate using RF and DC magnetron sputtering techniques, respectively. The device, which comprises 16 modules, is then encapsulated with a cellulose film. These f-TEGs can generate a power density of approximately 42 μW $cm^{-2}$ at a thermal gradient of 14 K, and this performance remains consistent even when the device is bent. Furthermore, its high-resolution sensing capabilities for temperature less than 0.19 K and velocity less than 0.03 cm $s^{-1}$ underscore its significant application prospect in the field of sensors.

### 3.2.3 Polyethylene naphthalate (PEN)

PEN film also emerges as an excellent substrate with great transparency and flexibility. As an example, Umeda and his team [142] designed f-TEGs by depositing an amorphous indium-gallium-zinc-oxide thin film onto a PEN substrate via magnetron sputtering technique. The f-TEGs features two legs connected in series through Au/Mo electrodes and Cu pads. An output voltage of ~6.7 mV and an output power of about 0.12 nW at a thermal gradient of 53 K could be obtained.

### 3.2.4 Mica

$Ca_3Co_4O_9$ is a non-toxic p-type TE material. Eklund's group [143] grew $Ca_3Co_4O_9$ films on mica substrates via multi-step sputtering, achieving a PF of ~1180 μW $m^{-1}$ $K^{-2}$ at 573 K. The films remained intact under tensile or compressive stress (r = 14 mm). Later, they deposited $Zn_{0.99}Ga_{0.01}O$ films on flexible mica using CVD, achieving a PF of ~100 μW $m^{-1}$ $K^{-2}$ at RT [144].

Recently, Zhong et al. [145] used one-step CVD to deposit polycrystalline SnSe on fluorphlogopite mica, obtaining highly oriented SnSe (400) films with a ZT of 0.15 at 550 K. A single-leg f-TEG produced 17 mV at a 50.5 K thermal gradient, and devices with varying units were designed for diverse applications.

### 3.2.5 Cellulose

Because of the biosafety and exceptional adaptability of cellulose, the TE textile-based generator which could maintain direct contact with human body garners significant focus. This innovative concept was recently proposed in a pioneering study [146]. Motivated by Kato's research [147], which reported the self-assembly of a porous structure, Jin and his team [44] utilized an unbalanced magnetron sputtering technique to prepare $Bi_2Te_3$ onto cellulose fiber (CF) paper. The strong scattering effect significantly enhanced S while reducing κ, resulting in a ZT of approximately

0.38 at 473 K. Notably, the $Bi_2Te_3$/CF film exhibited superior flexibility compared to the $Bi_2Te_3$/PI film. Furthermore, the researchers fabricated a novel TE device where one end of the strip was clamped with an alligator clip and the other end was held by fingers (as illustrated in **Figure 5n-o**). This generator, which featured 12 units of p-n legs, showed a stable voltage of 0.14 V with a thermal gradient of 50 K. Similar work was also reported by Rojas and his team [148]. The atomic layer deposition technique was employed by Karttunen and colleagues [149] to create ZnO-based films on cotton textile substrates. Among these, the $(Al_2O_3)_{50}(Zn_{0.99}Al_{0.01}O)_{600}$ film exhibited the PF of 137 μW $m^{-1}$ $K^{-2}$ at 300 K, with great flexibility.

*3.2.6 Carbon materials*

Till now, graphene is the most common carbon materials used as substrates for deposition due to its smaller lattice mismatch with TE materials [150]. It could greatly reduce residual stress during deposition process and prevents deformation, including wrinkling and warping. For instance, Lee and his team [151] deposited n-type ($Bi_2Te_3$) and p-type ($Sb_2Te_3$) films onto graphene using plasma-enhanced CVD. The deposited films exhibited excellent PFs at RT of 3520 μW $m^{-1}$ $K^{-2}$ (n-type) and 3590 μW $m^{-1}$ $K^{-2}$ (p-type) due to its high orientation along the (00 l) plane.

*3.2.7 Polyacrylonitrile (PAN)*

PAN is a polymer compound obtained by free radical polymerization of acrylonitrile. It possesses good resistance to chemical reagents, especially inorganic acids, bleaching powder, hydrogen peroxide, and general organic reagents. For instance, Lee and his colleagues [152] were the first to utilize an electrospinning method to create highly orientated PAN sheets, followed by depositing $Bi_2Te_3$ and $Sb_2Te_3$ onto these as-prepared PAN substrates to obtain a nanofiber structure. The resulting film demonstrated remarkable flexibility and exceptional tensile strength, with minimal changes in electrical resistance during stretching up to approximately 10.5% strain. These twist yarns were then fabricated into f-TEGs, with an output power density of 8.56 W $m^{-2}$ at a thermal gradient of 200 K.

### 3.3 Printing

Thanks to its streamlined processing steps, minimized material waste, low costs, and straightforward, printing technology has become exceptionally appealing and has advanced to enable the patterning of a diverse array of electronic materials onto various substrates. It mainly involves dispenser printing, screen printing, inkjet printing and 3D printing. The former two printing methods are widely used due to their convenience, are the most prevalent printing processes; however, they frequently lack precision and controllability. The latter two approaches address these deficiencies, albeit with relatively costly equipment.

*3.3.1 PI*

Zhang's research group has published several studies on the preparation of TE films using printing processes [54, 153–156]. Some of these studies focused on rigid substrates [154], while others were conducted on PI substrates. For example, in one study, they [153] first synthesized $Bi_2Te_{2.8}Se_{0.2}$ through

microwave-stimulated wet-chemical synthesis and then use screen printing technique to prepare it on a PI, followed by thermal treatment at 703 K to remove the surfactant and enhance film density. The high density (up to 85% relative density) and phonon scattering caused by nanoscale grains and pores resulted in a ZT value of 0.43 at 448 K. Later on, they tried to use different printing method to prepare Bi-Te alloys on PI substrate, like 3D conformal aerosol jet printing [156]. However, it seems that printing technique has little effect on TE performance while the processing technology of Bi-Te alloy raw materials and post-sintering process has more impact on the resulted film [54].

Additionally, Hou et al. [157] employed brush-printing to deposit $Bi_{0.5}Sb_{1.5}Te_3$/epoxy flexible films on a PI, with a hot-pressing treatment. Thanks to the preferential orientation of (000 l), the film showed an impressive PF of approximately 840 μW $m^{-1}$ $K^{-2}$ at RT, with excellent flexibility. When the current was set at 60 mA, an f-TEG with eight elements generated a thermal gradient of 6.2 K, surpassing previously reported $Bi_2Te_3$-based cooling devices [158–160]. Similar work was also reported in Chen et al. [161]. Most recently, Du et al. [162] fabricated several types of chalcogenide nanowires based-inks and then utilized ink printing method to prepared $Ag_2Te$-based f-TEFs on glass fiber, which exhibited a PF of 493.8 μW $m^{-1}$ $K^{-2}$ at 400 K, and the resulted f-TEGs showed a maximum power density of 0.9 μW $cm^{-2}$ $K^{-2}$.

### *3.3.2 Cellulose*

Ferhat et al. [163] utilized inkjet printing to prepare a $TiS_2$-based component on a flexible paper substrate, with a post heat-treatment at a temperature range of 383–388 K. By optimizing the hexylammonium content, a maximum PF of 210 μW $m^{-1}$ $K^{-2}$ could be obtained. f-TEGs with 7 units could generate a power density of 17.6 μW $cm^{-2}$ at a thermal gradient of 20 K.

More recently, Zhao et al. [164] developed TE ink containing $Bi_2Te_3$ and bacterial cellulose nanofibers, enhanced with an alkyl ketene dimer emulsion to improve adhesion and water resistance. The resulted honeycomb-like generator with 96 pair of p-n legs could generate a $V_{voltage}$ of 70.5 mV and a maximum P of 596 nW at a thermal gradient of 55 K. In Ref. [165], untreated paper served as the substrate for p-type ($Bi_2Se_{0.3}Te_{2.7}$) and n-type ($Bi_{0.5}Sb_{1.5}Te_3$) legs, fabricated via modified dispenser printing to form a f-TEG. With ten legs, the f-TEG produced 8 mV and 10 nW of power under a 35 K thermal gradient. Similar work was also reported in Shin et al. [166].

When considering printing techniques for TE materials, the following suggestions are offered: (a) When preparing the slurry, it is advisable to select a binder with a lower melting point and gasification temperature, to ensure its positive role in recrystallization annealing and minimize residual binder during heat treatment. (b) The ink's contact angle should be greater than 40° but less than 90° to ensure accurate pattern reproduction during the printing process. (c) For substrates with a rough surface, such as glass fiber, a pre-coating of a polymer like chitosan may be necessary to facilitate proper ink adhesion and pattern formation.

## 3.4 Coating

Coating is also a convenient technique utilized for forming films, encompassing spin coating, roll coating, drop casting, spray coating, and dip coating (**Figure 6**).

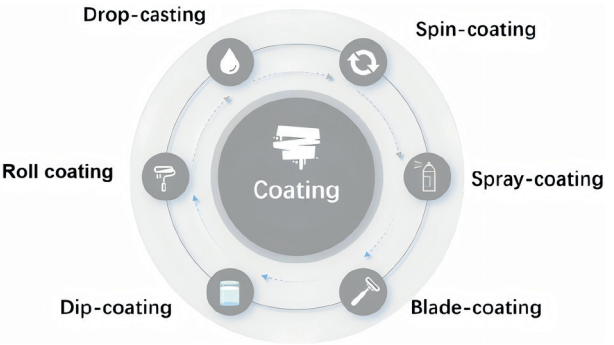


**Figure 6.**
*The classification of coating technology.*

### *3.4.1 PI*

Takashiri's team [167] synthesized hexagonal $Bi_2Te_3$ nanoplates via solvothermal method and drop-cast them onto a PI substrate. After refining thermal annealing, they [168] achieved a maximum PF of ~350 μW $m^{-1}$ $K^{-2}$ at RT. They then applied the same method to prepare n-type $Bi_2(Se_xTe_{1-x})_3$ films, reaching a PF of ~410 μW $m^{-1}$ $K^{-2}$ at RT for $Bi_2(Se_{0.75}Te_{0.25})_3$.

In addition to inorganics, numerous works have tried to drop-cast CPs on PI substrates. For example, Bharti et al. [169] drop-cast PEDOT:PSS-based solutions onto PI substrates, followed by annealing. A full-organic f-TEGs with 30 legs generated an U of approximately 17.6 mV and an P of approximately 207 nW at a thermal gradient of 80 K.

Bulk $Cu_2Se$ also exhibits excellent TE performance [170]. Consequently, Lin et al. [171] prepared $Cu_2Se$-based ink and then deposited onto a flexible PI substrate through spin coating, with a post-annealing at a temperature around 573–773 K. The resulted film exhibited a PF of approximately 460 μW $m^{-1}$ $K^{-2}$ at 664 K, which represents the highest value reported for $Cu_2Se$-based f-TEFs.

### *3.4.2 PET*

Layer-by-layer self-assembly is a process by which composite membranes are constructed through alternating deposition of specific polymers, quantum dots, nanoparticles, biomolecules, and other substances, under the action of complementary interactions such as electrostatic interaction, hydrogen bonding, coordination bonding, and covalent bonding. Cho's group utilized this approach to fabricate organic TE films on PET substrates using dip-coating. They [172] successfully prepared a multiple-layered CP-carbon composite (PANi/graphene-PEDOT:PSS/PANi/DWCNT-PEDOT:PSS) film on a PET substrate. The composite film exhibited a PF of ~2710 μW $m^{-1}$ $K^{-2}$ at RT.

Tian et al. [173] used NMP to exfoliate $TiS_2$ powder into nanosheets, intercalated hexylamine to form a hybrid superlattice film, and dip-coated it onto a UV-treated PET substrate, achieving a PF of ~210 μW $m^{-1}$ $K^{-2}$ at RT. Choi et al. [174] synthesized SnSe nanosheets via hydrothermal synthesis, drop-casting them onto a PET substrate. The film showed an out-of-plane S of ~1250 μV $K^{-1}$), much higher than SnSe single crystals (809 μV $K^{-1}$), likely due to carrier filtering, despite a low σ of 2.4 S $cm^{-1}$.

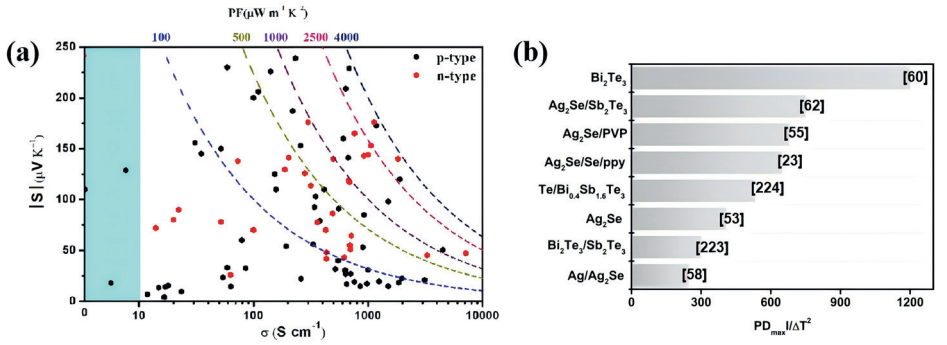


**Figure 7.**
*(a) Selected PFs and corresponding σ and S of the f-TEFs reported in literatures. The blue region represents areas with very low PF values, indicating material systems that are not worth exploring in the future. The dashed lines in different colors correspond to the PF values at their respective peaks. Black dots represent p-type TE materials, while red dots represent n-type TE materials. Image reproduced with permission from Ref. [72] published by Elsevier. (b) Selected normalized maximum powder density ($PD_{max}l/\Delta T^2$) in high-performance f-TEGs [23, 53, 55, 58, 60, 62, 176–179].*

### *3.4.3 Poly-p-phenylene terephthamide (PPTA)*

Jang et al. [175] employed the mechanical alloying technique to synthesize BiSbTe alloy particles and subsequently incorporated nanofiber cellulose as a binder to formulate a mixed paste. This paste was then drop-cast onto chitosan-precoated PPTA, followed by cold pressing (**Figure 7e**). By refining the composition, a sample containing $Bi_{0.46}Sb_{1.34}Te_{3.2}$ after pressing treatment, showed a peak PF of approximately 611 μW $m^{-1}$ $K^{-2}$ at RT.

Apart from the aforementioned substrates, other materials, such as glass fiber, have been utilized for coating purposes. The coating technique is advantageous in terms of convenience, speed, and environmentally friendly method. However, the TE performance of the resulting films typically remains modest.

## 4. Challenge and prospective

### 4.1 TE property measurement

### *4.1.1 Electrical conductivity*

Electrical conductivity, a well-established property that might initially seem redundant to mention, presents unique challenges when measured in TE films, beyond those encountered in bulks. Conventionally, the four-probe method is employed to test σ of films, necessitating an accurate determination of film thickness. For freestanding TE films, thickness measurement is straightforward; however, for films deposited on substrates, this task becomes more intricate, particularly if the substrate has an uneven surface or a porous structure, like glass fiber, which can significantly impact the film's thickness.

To address this issue, enhancing the substrate's surface smoothness, such as through pre-coating with chitosan, can be beneficial [175]. Furthermore, ensuring uniform film deposition, for instance, by using a homogeneously dispersed precursor solution during vacuum filtration, is crucial. Selecting an appropriate method

for thickness measurement is also vital. Observing the sample's cross-section under scanning electron microscopy (SEM) is a common and intuitive approach, where preparing a clear cross-section is pivotal. Brittle fracture of samples in liquid nitrogen is a standard technique for obtaining such cross-sections. However, when cellulose-based materials, like nylon, serve as substrates, even this method may fail to produce a clean break. In such cases, employing a knife-assisted liquid nitrogen brittle fracture method, as detailed in the supporting information of refs. [50, 53], can be helpful.

Lastly, to enhance measurement accuracy, it is advisable to observe as wide a field as possible under SEM, measure numerous points, and average the data.

#### *4.1.2 In-plane thermal conductivity*

Measuring the in-plane κ of a film remains a significant challenge to this day. Three primary methods have been reported for this purpose [180]. The first involves using the LINSEIS TFA apparatus that operates based on the 3ω-method. Nevertheless, this approach necessitates depositing the film on a specialized substrate, thereby limiting its broad applicability. The second method employs a suspended microdevice that consists of two adjacent $SiN_x$ membranes. Each membrane is adorned with a serpentine platinum resistance thermometer, accompanied by two electrodes and six supporting beams, enabling the conduction of four-probe measurements of TE properties [181]. While sophisticated, this method also presents its own set of challenges. The third method employs the Laser-Flash technique to measure in-plane thermal diffusivity (D). By combining this with the film's density (ρ) and specific heat capacity at constant pressure (Cp), the thermal conductivity (κ) can be calculated using the equation: $\kappa = \rho C_p D$. Details of this calculation are provided in the supporting information of reference [53]. However, a limitation of this method is that it requires a relatively large film size. For freestanding f-TEFs, this method can directly yield the in-plane thermal conductivity. The fourth method is called transient electro-thermal (TET) technique, which is an approach with high accuracy to measure the thermal diffusivity of various solid materials. In a typical TET measurement, the sample is suspended between two electrodes, where the electrodes also serve as heat sink during the thermal transport characterization and this method was proved to be accurate by the measurement of some freestanding films [60]. Yet, for f-TEFs deposited on substrates, the measured in-plane thermal conductivity inevitably includes contributions from the substrate, posing a challenge in isolating the thermal conductivity of the TE film itself.

#### *4.1.3 Seebeck coefficient*

While measuring the Seebeck coefficient may seem straightforward, it is crucial to remember that this coefficient is determined by the slope of the linear relationship between the thermal electromotive force and the temperature difference (ranging from approximately 2–5 K) between the two ends of a film. Given that the value of ZT is in proportional to the square of the S, any inaccuracies in measuring S can pose significant issues, particularly for materials with low S, like CP and carbon materials.

### 4.2 f-TEGs

Currently, the research on f-TEGs is still in the nascent stages of principle demonstration, lagging significantly behind the advancements made in the field of f-TEFs. Hence, it is imperative to intensify efforts in studying f-TEGs.

In the case of f-TEGs, the legs are constructed from thin films, distinguishing them vastly from devices made of bulk TE materials. For identical materials and TE leg lengths, the resistance of thin films is several hundred times greater than that of bulk materials. Furthermore, the electrical power generated by f-TEGs typically falls within the micro-watt range, necessitating amplification via a chip equipped with DC/DC amplification and capacitor storage for practical use. Consequently, if the $R_{in}$ of f-TEGs is excessively high, the V drop across the f-TEGs will be substantial, resulting in an insufficient voltage supplied to the chip, thereby hindering power generation or even preventing the chip from triggering. To address this, researchers should endeavor to produce thicker TE films and select material systems with higher electrical conductivity.

To minimize contact resistance, the ends of each leg should be sputtered with electrodes, such as gold. It is worth noting that silver electrodes, while commonly used, are prone to aging in air at room temperature. Therefore, if silver electrodes are utilized, the device must be adequately packaged to prevent degradation.

### 4.3 Summary

To sum up, we have provided an in-depth examination of f-TEFs, focusing on two distinct aspects: freestanding f-TEFs and substrate-based f-TEFs, and based on our review, we propose the following outlooks:

1. In case of freestanding TE films, the integration of room-temperature metal-like plasticity with adjustable bandgaps and high carrier mobility to create plastic inorganic semiconductors remains a promising direction for future exploration. For instance, utilizing anti-situ defects to transform brittle materials into plastic materials has been proven to be an effective strategy. Meanwhile, it is essential to explore more cost-effective methods for slicing bulk materials into films, as this is crucial for future large-scale production. In terms of f-TEFs based on substrates, post-treatment often significantly affects the TE performance of thin films, while the physical properties of the substrate often constrain the overall post-treatment process of the samples. For instance, in the post-treatment of certain thin films, higher heat treatment temperatures can significantly enhance film performance, necessitating substrates with higher melting points. Consequently, substrates with specific properties, such as high-temperature-resistant PDMS or highly flexible PPTA, deserve greater attention (see **Table 1**).

2. As shown in Eq. 4, the PF of f-TEFs is directly proportional to the maximum power density of f-TEGs. Consequently, achieving superior output performance in f-TEGs requires a higher PF.

   **Figure 7a** presents typical data on PF, along with corresponding $\sigma$ and $S$ values, for f-TEFs reported in various literature sources. As observed in **Figure 7a**, high PF values are generally achieved when σ exceeds 1000 S/cm, and the value of S varies between 100 and 250 μV/K.

3. Early research on TE generators primarily focused on applications in power generation through temperature difference. In recent years, TE devices have also been explored in various other fields, such as temperature sensors [225], fire alarms [226], and gesture recognition [227]. Furthermore, TE conversion tech-

| Type of substrate | Molecular structure | Electrical conductivity (S $cm^{-1}$) | Thermal conductivity ($W{\cdot}m^{-1}{\cdot}K^{-1}$) | Melting point (°C) | Tensile strength (MPa) |
|---|---|---|---|---|---|
| Nylon membrane | 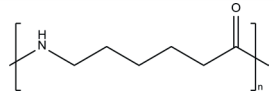 | $10^{-15}$ [180] | 0.24 [181] | 268.46 [182] | 304 [183] |
| PVDF membrane | 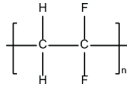 | ≈$10^{-12}$ [184] | 0.25 [185] | 156.5–162.3 [186] | 50 [187] |
| PTFE membrane | 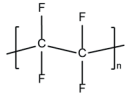 | 5.1x$10^{-19}$ [188] | 0.27 [189] | 331 [190] | 7.52 [191] |
| PI | 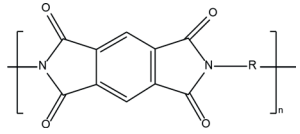 | $10^{-16}$ [192] | 0.27 [193] | >400 [194] | 1562 [195] |
| PET | 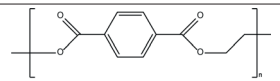 | $10^{-14}$ [196] | 0.19 [181] | 250–255 [197] | 998 [198] |
| PEN | 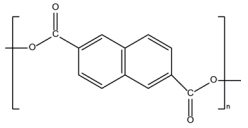 | Unknown | 0.26 [199] | 265 [200] | 200 [201] |
| PAN | 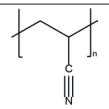 | 5x$10^{-8}$ [202] | 0.01–0.06 [203] | 135 [204] | 1800 [205] |
| Mica | $K(Mg,Fe,Al)_3(Si,Al)_4O_{10}(OH,F)_2$ | $10^{-12}$ [206] | 0.1 [207] | 700 [143] | 32 [208] |

| Type of substrate | | Molecular structure | Electrical conductivity (S cm$^{-1}$) | Thermal conductivity (W·m$^{-1}$·K$^{-1}$) | Melting point (°C) | Tensile strength (MPa) |
|---|---|---|---|---|---|---|
| Cellulose | Paper | 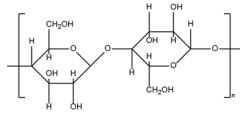 | $10^{-6}$ [209] | 0.029–0.17 [210] | 450 [211] | 34 [212] |
| | Cotton | | | 0.071 [210] | 450 [211] | 128–597 [213] |
| Carbon materials | CNT | / | 5.15 [214] | 2000 [215] | 4527 [216] | 43,000 [217] |
| | Graphene | 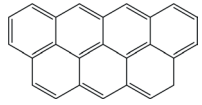 | 59 [218] | 3080–5100 [219] | 4727 [220] | 150 [218] |
| PPTA | | 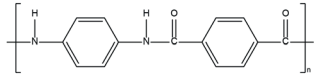 | $10^{-9}$ [221] | 0.023–0.04 [222] | 550 [223] | 3600 [224] |

**Table 1.**
*Typical physical properties of substrates for the preparation of f-TEFs.*

nology, based on the Peltier effect of semiconductor materials, enables localized heat transport and active cooling in confined spaces. With features like miniaturization, fast response, and ease of integration, it has been tested for applications such as chip cooling [228]. Future research on TE devices could place greater emphasis on these emerging applications.

4. Considering that the f-TEGs designed are intended for applications near RT, it is advisable to opt for materials that exhibit high TE performance around RT, such as $Ag_2Se$ and $Bi_2Te_3$, as the target material for the inorganic component. Meanwhile, the currently reported high-performance f-TEGs are concentrated within these two material systems (**Figure 7b**). Also, more room-temperature TE materials should be given attention, such as $Mg_2Sb_3$-based materials.

5. Inorganic materials generally outperform organic ones in TE properties, making it essential to maximize their content in organic/inorganic composite films. However, the chemical disparity between components complicates achieving seamless interfaces. In situ synthesis of core/shell nanostructures and hybrid films offers a promising solution [50, 55].

We hope that this chapter provides valuable guidance for the preparation of high-performance f-TEFs, processing strategies, and f-TEGs design, ultimately contributing to the advancement and practical application of f-TEGs.

## Acknowledgements

This chapter was supported by the National Natural Science Foundation of China (NSFC) (Grant no. 52402232), Guangdong Basic and Applied Basic Research Foundation (Grant no. 2023A1515110512), Southern University of Science and Technology (Grant no. Y01796223), and the open research fund of Songshan Lake Materials Laboratory (Grant no. 2023SLABFN15).

## Conflict of interest

There are no conflicts of interest to declare.

## Notes/thanks/other declarations

Special thanks are due to Prof. Kefeng Cai for his valuable comments.

## Author details

Xiang Li and Yao Lu*
School of Microelectronics, Southern University of Science and Technology, Shenzhen, China

*Address all correspondence to: luy8@sustech.edu.cn

IntechOpen

## References

[1] Wortmann F, Flüchter K. Internet of things: technology and value added. Business & Information Systems Engineering. 2015;**57**:221-224. DOI: 10.1007/s12599-015-0383-3

[2] Haras M, Skotnicki T. Thermoelectricity for IoT–A review. Nano Energy. 2018;**54**:461-476. DOI: 10.1016/j.nanoen.2018.10.013

[3] Madakam S, Ramaswamy R, Tripathi S. Internet of Things (IoT): A literature review. Journal of Computer and Communications. 2015;**3**:164-173. DOI: 10.4236/jcc.2015.35021

[4] Idhalama OU, Oredo JO. Exploring the next generation Internet of Things (IoT) requirements and applications: A comprehensive overview. Information Development. 2024:02666669241267852. DOI: 10.1177/02666669241267852

[5] Nozariasbmarz A, Collins H, Dsouza K, Polash MH, Hosseini M, Hyland M, et al. Review of wearable thermoelectric energy harvesting: From body temperature to electronic systems. Applied Energy. 2020;**258**:114069. DOI: 10.1016/j.apenergy.2019.114069

[6] Kanahashi K, Pu J, Takenobu T. 2D materials for large-area flexible thermoelectric devices. Advanced Energy Materials. 2020;**10**:1902842. DOI: 10.1002/aenm.201902842

[7] Lin MC, Gong M, Lu B, Wu Y, Wang DY, Guan M, et al. An ultrafast rechargeable aluminium-ion battery. Nature. 2015;**520**:324-328. DOI: 10.1038/nature14340

[8] Ponrouch A, Frontera C, Bardé F, Palacín MR. Towards a calcium-based rechargeable battery. Nature Materials. 2016;**15**:169-172. DOI: 10.1038/nmat4462

[9] Wang Y, Yang L, Shi XL, Shi X, Chen L, Dargusch MS, et al. Flexible thermoelectric materials and generators: challenges and innovations. Advanced Materials. 2019;**31**:1807916. DOI: 10.1002/adma.201807916

[10] Siddique ARM, Mahmud S, Van B. A review of the state of the science on wearable thermoelectric power generators (TEGs) and their existing challenges. Renewable and Sustainable Energy Reviews. 2017;**73**:730-744. DOI: 10.1016/j.rser.2017.01.177

[11] Scrosati B, Hassoun J, Sun YK. Lithium-ion batteries. A look into the future. Energy & Environmental Science. 2011;**4**:3287-3295. DOI: 10.1039/C1EE01388B

[12] Lechêne BP, Cowell M, Pierre A, Evans JW, Wright PK, Arias AC. Organic solar cells and fully printed super-capacitors optimized for indoor light energy harvesting. Nano Energy. 2016;**26**:631-640. DOI: 10.1016/j.nanoen.2016.06.017

[13] Zhao W, Liu Z, Sun Z, Zhang Q, Wei P, Mu X, et al. Superparamagnetic enhancement of thermoelectric performance. Nature. 2017;**549**:247-251. DOI: 10.1038/nature23667

[14] Chen Z, Jian Z, Li W, Chang Y, Ge B, Hanus R, et al. Lattice dislocations enhancing thermoelectric PbTe in addition to band convergence. Advanced Materials. 2017;**29**:1606768. DOI: 10.1002/adma.201606768

[15] Zhu T, Liu Y, Fu C, Heremans JP, Snyder JG, Zhao X. Compromise and synergy in high-efficiency thermoelectric materials. Advanced Materials. 2017;**29**:1605884. DOI: 10.1002/adma.201605884

[16] Wu Y, Nan P, Chen Z, Zeng Z, Liu R, Dong H, et al. Thermoelectric enhancements in PbTe alloys due to dislocation-induced strains and converged bands. Advanced Science. 2020;**7**:1902628. DOI: 10.1002/advs.201902628

[17] Zhao LD, Lo SH, Zhang Y, Sun H, Tan G, Uher C, et al. Ultralow thermal conductivity and high thermoelectric figure of merit in SnSe crystals. Nature. 2014;**508**:373-377. DOI: 10.1038/nature13184

[18] Wang J, Cai K, Shen S. A facile chemical reduction approach for effectively tuning thermoelectric properties of PEDOT films. Organic Electronics. 2015;**17**:151-158. DOI: 10.1016/j.orgel.2014.12.007

[19] Wang J, Cai K, Shen S. Enhanced thermoelectric properties of poly (3, 4-ethylenedioxythiophene) thin films treated with $H_2SO_4$. Organic Electronics. 2014;**15**:3087-3095. DOI: 10.1016/j.orgel.2014.09.012

[20] Li Y, Du Y, Dou Y, Cai K, Xu J. PEDOT-based thermoelectric nanocomposites–A mini-review. Synthetic Metals. 2017;**226**:119-128. DOI: 10.1016/j.synthmet.2017.02.007

[21] Wu J, Sun Y, Xu W, Zhang Q. Investigating thermoelectric properties of doped polyaniline nanowires. Synthetic Metals. 2014;**189**:177-182. DOI: 10.1016/j.synthmet.2014.01.007

[22] Yao Q, Chen L, Xu X, Wang C. The high thermoelectric properties of conducting polyaniline with special submicron-fibre structure. Chemistry Letters. 2015;**34**:522-523. DOI: 10.1246/cl.2005.522

[23] Li Y, Lou Q, Yang J, Cai K, Liu Y, Lu Y, et al. Exceptionally high power factor $Ag_2Se$/Se/polypyrrole composite films for flexible thermoelectric generators. Advanced Functional Materials. 2022;**32**:2106902. DOI: 10.1002/adfm.202106902

[24] Tong L, Gao M, Jiang C, Cai K. Ultra-high performance and flexible polypyrrole coated CNT paper electrodes for all-solid-state supercapacitors. Journal of Materials Chemistry A. 2019;**7**:10751-10760. DOI: 10.1039/C9TA01856E

[25] Xu S, Shi XL, Dargusch M, Di C, Zou J, Chen ZG. Conducting polymer-based flexible thermoelectric materials and devices: from mechanisms to applications. Progress in Materials Science. 2021;**121**:100840. DOI: 10.1016/j.pmatsci.2021.100840

[26] Kim N, Lienemann S, Petsagkourakis I, Alemu D, Kee S, Ederth T, et al. Elastic conducting polymer composites in thermoelectric modules. Nature Communications. 2020;**11**:1424. DOI: 10.1038/s41467-020-15135-w

[27] Bharti M, Singh A, Samanta S, Aswal DK. Conductive polymers for thermoelectric power generation. Progress in Materials Science. 2018;**93**:270-310. DOI: 10.1016/j.pmatsci.2017.09.004

[28] Qin J, Du Y, Wang L, Du M, Eklund P, Ke Q. Flexible two-dimensional inorganic nanosheet/PEDOT: PSS thermoelectric composite films. Energy Material Advances. 2024;**5**:0097. DOI: 10.34133/energymatadv.0097

[29] Jiang Q, Pan D, Wang Y, Liu Y, Luo Y, Yang J, et al. High thermoelectric performance related to PVDF ferroelectric domains in p-type flexible PVDF-$Bi_{0.5}Sb_{1.5}Te_3$ composite film.

Small. 2024;**20**:2306786. DOI: 10.1002/smll.202306786

[30] Nie X, Ke S, Zhang H, Xu W, Li X, Wei P, et al. Enhancing electrical properties of flexible BiSbTe/epoxy composite films via liquid-phase extrusion. Journal of Power Sources. 2024;**623**:235405. DOI: 10.1016/j.jpowsour.2024.235405

[31] Du Y, Chen J, Meng Q, Xu J, Paul B, Eklund P. Flexible ternary carbon black/$Bi_2Te_3$ based alloy/polylactic acid thermoelectric composites fabricated by additive manufacturing. Journal of Materiomics. 2020;**6**:293-299. DOI: 10.1016/j.jmat.2020.02.010

[32] Du Y, Chen J, Meng Q, Dou Y, Xu J, Shen SZ. Thermoelectric materials and devices fabricated by additive manufacturing. Vacuum. 2020;**178**:109384. DOI: 10.1016/j.vacuum.2020.109384

[33] Meng Q, Qiu Y, Cai K, Ding Y, Wang M, Pu H, et al. High performance and flexible polyvinylpyrrolidone/Ag/$Ag_2Te$ ternary composite film for thermoelectric power generator. ACS Applied Materials & Interfaces. 2019;**11**:33254-33262. DOI: 10.1021/acsami.9b11217

[34] Rincón-García L, Ismael AK, Evangeli C, Grace I, Rubio-Bollinger G, Porfyrakis K, et al. Molecular design and control of fullerene-based bi-thermoelectric materials. Nature Materials. 2016;**15**:289-293. DOI: 10.1038/nmat4487

[35] El-Shamy AG. The role of nitrogen-carbon dots (NC) nano-particles in enhancing thermoelectric power functions of PEDOT: PSS/Te nano-composite films. Chemical Engineering Journal. 2021;**417**:129212. DOI: 10.1016/j.cej.2021.129212

[36] Wei S, Zhang Y, Lv H, Deng L, Chen G. SWCNT network evolution of PEDOT: PSS/SWCNT composites for thermoelectric application. Chemical Engineering Journal. 2022;**428**:131137. DOI: 10.1016/j.cej.2021.131137

[37] Xia B, Shi XL, Zhang L, Luo J, Chen WY, Hu B, et al. Vertically designed high-performance and flexible thermoelectric generator based on optimized PEDOT: PSS/SWCNTs composite films. Chemical Engineering Journal. 2024;**486**:150305. DOI: 10.1016/j.cej.2024.150305

[38] El-Shamy AG. Review on the recent advance in PEDOT: PSS/Carbonic fillers based nanocomposite for flexible thermoelectric devices and sensors. Materials Today Physics. 2023;**35**:101101. DOI: 10.1016/j.mtphys.2023.101101

[39] Bae EJ, Kang YH, Lee C, Cho SY. Engineered nanocarbon mixing for enhancing the thermoelectric properties of a telluride-PEDOT: PSS nanocomposite. Journal of Materials Chemistry A. 2017;**5**:17867-17873. DOI: 10.1039/C7TA04280A

[40] Yoo D, Kim J, Lee SH, Cho W, Choi HH, Kim FS, et al. Effects of one-and two-dimensional carbon hybridization of PEDOT: PSS on the power factor of polymer thermoelectric energy conversion devices. Journal of Materials Chemistry A. 2015;**3**:6526-6533. DOI: 10.1039/C7TA04280A

[41] Taroni PJ, Santagiuliana G, Wan K, Calado P, Qiu M, Zhang H, et al. Toward stretchable self-powered sensors based on the thermoelectric response of PEDOT: PSS/polyurethane blends. Advanced Functional Materials. 2018;**28**:1704285. DOI: 10.1002/adfm.201704285

[42] Zhang Y, Zhang Q, Chen G. Carbon and carbon composites for

thermoelectric applications. Carbon Energy. 2020;**2**:408-436. DOI: 10.1002/cey2.68

[43] Wang L, Zhang Z, Liu Y, Wang B, Fang L, Qiu J, et al. Exceptional thermoelectric properties of flexible organic– inorganic hybrids with monodispersed and periodic nanophase. Nature Communications. 2018;**9**:3817. DOI: 10.1038/s41467-018-06251-9

[44] Jin Q, Shi W, Zhao Y, Qiao J, Qiu J, Sun C, et al. Cellulose fiber-based hierarchical porous bismuth telluride for high-performance flexible and tailorable thermoelectrics. ACS Applied Materials & Interfaces. 2018;**10**:1743-1751. DOI: 10.1021/acsami.7b16356

[45] Kim SH, Min T, Choi JW, Baek SH, Choi JP, Jr C. Ternary $Bi_2Te_3In_2Te_3Ga_2Te_3$ (n-type) thermoelectric film on a flexible PET substrate for use in wearables. Energy. 2018;**144**:607-618. DOI: 10.1016/j.energy.2017.12.063

[46] Li T, Pickel AD, Yao Y, Chen Y, Zeng Y, Lacey SD, et al. Thermoelectric properties and performance of flexible reduced graphene oxide films up to 3,000 K. Nature Energy. 2018;**3**:148-156. DOI: 10.1038/s41560-018-0086-3

[47] Jin Q, Jiang S, Zhao Y, Wang D, Qiu J, Tang DM, et al. Flexible layer-structured $Bi_2Te_3$ thermoelectric on a carbon nanotube scaffold. Nature Materials. 2019;**18**:62-68. DOI: 10.1038/s41563-018-0217-z

[48] Ding Y, Qiu Y, Cai K, Yao Q, Chen S, Chen L, et al. High performance n-type $Ag_2Se$ film on nylon membrane for flexible thermoelectric power generator. Nature Communications. 2019;**10**:841. DOI: 10.1038/s41467-019-08835-5

[49] Liang J, Wang T, Qiu P, Yang S, Ming C, Chen H, et al. Flexible thermoelectrics: from silver chalcogenides to full-inorganic devices. Energy & Environmental Science. 2019;**12**:2983-2990. DOI: 10.1039/C9EE01777A

[50] Lu Y, Qiu Y, Cai K, Ding Y, Wang M, Jiang C, et al. Ultrahigh power factor and flexible silver selenide-based composite film for thermoelectric devices. Energy & Environmental Science. 2020;**13**:1240-1249. DOI: 10.1039/C9EE01609K

[51] Lu Y, Qiu Y, Cai K, Li X, Gao M, Jiang C, et al. Ultrahigh performance PEDOT/$Ag_2Se$/CuAgSe composite film for wearable thermoelectric power generators. Materials Today Physics. 2020;**14**:100223. DOI: 10.1016/j.mtphys.2020.100223

[52] He S, Li Y, Liu L, Jiang Y, Feng J, Zhu W, et al. Semiconductor glass with superior flexibility and high room temperature thermoelectric performance. Science Advances. 2020;**6**:eaaz8423. DOI: 10.1126/sciadv.aaz8423

[53] Jiang C, Ding Y, Cai K, Tong L, Lu Y, Zhao W, et al. Ultrahigh performance of n-type $Ag_2Se$ films for flexible thermoelectric power generators. ACS Applied Materials & Interfaces. 2020;**12**:9646-9655. DOI: 10.1021/acsami.9b21069

[54] Varghese T, Dun C, Kempf N, Saeidi-Javash M, Karthik C, Richardson J, et al. Flexible thermoelectric devices of ultrahigh power factor by scalable printing and interface engineering. Advanced Functional Materials. 2020;**30**:1905796. DOI: 10.1002/adfm.201905796

[55] Jiang C, Wei P, Ding Y, Cai K, Tong L, Gao Q, et al. Ultrahigh performance polyvinylpyrrolidone/$Ag_2Se$ composite thermoelectric film

for flexible energy harvesting. Nano Energy. 2021;**80**:105488. DOI: 10.1016/j.nanoen.2020.105488

[56] Lei Y, Qi R, Chen M, Chen H, Xing C, Sui F, et al. Microstructurally tailored thin β-$Ag_2Se$ films toward commercial flexible thermoelectrics. Advanced Materials. 2022;**7**:2104786. DOI: 10.1002/adma.202104786

[57] Gao Z, Yang Q, Qiu P, Wei T, Yang S, Xiao J, et al. p-type plastic inorganic thermoelectric materials. Advanced Energy Materials. 2021;**11**:2100883. DOI: 10.1002/aenm.202100883

[58] Li X, Lu Y, Cai K, Gao M, Li Y, Wang Z, et al. Exceptional power factor of flexible Ag/$Ag_2Se$ thermoelectric composite films. Chemical Engineering Journal. 2022;**434**:134739

[59] Yang Q, Yang S, Qiu P, Peng L, Wei T, Zhang Z, et al. Flexible thermoelectrics based on ductile semiconductors. Science. 2022;**377**:854-858. DOI: 10.1126/science.abq0682

[60] Lu Y, Zhou Y, Wang W, Hu M, Huang X, Mao D, et al. Staggered-layer-boosted flexible $Bi_2Te_3$ films with high thermoelectric performance. Nature Nanotechnology. 2023;**18**:1281-1288. DOI: 10.1038/s41565-023-01457-5

[61] Zheng ZH, Shi XL, Ao DW, Liu W, Meng L, Kou L, et al. Harvesting waste heat with flexible $Bi_2Te_3$ thermoelectric thin film. Nature Sustainability. 2023;**6**:180-191. DOI: 10.1038/s41893-022-01003-6

[62] Yang D, Shi XL, Li M, Nisar M, Mansoor A, Chen S, et al. Flexible power generators by $Ag_2Se$ thin films with record-high thermoelectric performance. Nature Communications. 2024;**15**:923. DOI: 10.1038/s41467-024-45092-7

[63] Suarez F, Nozariasbmarz A, Vashaee D, Öztürk MC. Designing thermoelectric generators for self-powered wearable electronics. Energy & Environmental Science. 2016;**9**:2099-2113. DOI: 10.1039/C6EE00456C

[64] Feng M, Lv S, Deng J, Guo Y, Wu Y, Shi G, et al. An overview of environmental energy harvesting by thermoelectric generators. Renewable and Sustainable Energy Reviews. 2023;**187**:113723. DOI: 10.1016/j.rser.2023.113723

[65] He J, Li K, Jia L, Zhu Y, Zhang H, Linghu J. Advances in the applications of thermoelectric generators. Applied Thermal Engineering. 2024;**236**:121813. DOI: 10.1016/j.applthermaleng.2023.121813

[66] Soleimani Z, Zoras S, Ceranic B, Cui Y, Shahzad S. A comprehensive review on the output voltage/power of wearable thermoelectric generators concerning their geometry and thermoelectric materials. Nano Energy. 2021;**89**:106325. DOI: 10.1016/j.nanoen.2021.106325

[67] Freer R, Powell AV. Realising the potential of thermoelectric technology: A Roadmap. Journal of Materials Chemistry C. 2020;**8**:441-463. DOI: 10.1039/C9TC05710B

[68] Gürkan K, Karaman H, Ballikaya S. Optimization of high-performance flexible thermoelectric generator from material synthesis to simulation and device application. Energy Conversion and Management. 2023;**291**:117335. DOI: 10.1016/j.enconman.2023.117335

[69] Masoumi S, O'Shaughnessy S, Pakdel A. Organic-based flexible thermoelectric generators: From materials to devices. Nano Energy. 2022;**92**:106774. DOI: 10.1016/j.nanoen.2021.106774

[70] Zhou Q, Li H, Du C, Ye Z, Liang L, Chen G. High-performance flexible thermoelectric generators with tunable in-plane and out-of-plane architectures. Nano Energy. 2023;**118**:109007. DOI: 10.1016/j.nanoen.2023.109007

[71] Dong Z, Liu H, Yang X, Fan J, Bi H, Wang C, et al. Facile fabrication of paper-based flexible thermoelectric generator. npj Flexible Electronics. 2021;**5**:6. DOI: 10.1038/s41528-021-00103-1

[72] Li X, Cai K, Gao M, Du Y, Shen S. Recent advances in flexible thermoelectric films and devices. Nano Energy. 2021;**89**:106309. DOI: 10.1016/j.nanoen.2021.106309

[73] Liu Y, Li Y, Wu M, Lu Y, Wang Z, Wei P, et al. Nanoengineering approach toward high power factor $Ag_2Se$/Se composite films for flexible thermoelectric generators. ACS Applied Materials & Interfaces. 2023;**15**:36587-36593. DOI: 10.1021/acsami.3c06960

[74] Zhou Q, Zhu K, Li J, Li Q, Deng B, Zhang P, et al. Leaf-inspired flexible thermoelectric generators with high temperature difference utilization ratio and output power in ambient air. Advanced Science. 2021;**8**:2004947. DOI: 10.1002/advs.202004947

[75] Lu Y, Han X, Wei P, Liu Y, Wang Z, Zuo X, et al. Nanoengineering approach toward ultrahigh power factor $Ag_2Se$/polyvinylpyrrolidone composite film for flexible thermoelectric generator. Chemical Engineering Journal. 2024;**485**:149793. DOI: 10.1016/j.cej.2024.149793

[76] Lu Y, Li X, Cai K, Gao M, Zhao W, He J, et al. Enhanced-performance PEDOT: PSS/$Cu_2Se$-based composite films for wearable thermoelectric power generators. ACS Applied Materials & Interfaces. 2021;**13**:631-638. DOI: 10.1021/acsami.0c18577

[77] Zhang J, Zhang W, Wei H, Tang J, Li D, Xu D. Flexible micro thermoelectric generators with high power density and light weight. Nano Energy. 2023;**105**:108023. DOI: 10.1016/j.nanoen.2022.108023

[78] Qiu P, Deng T, Chen L, Shi X. Plastic inorganic thermoelectric materials. Joule. 2024;**8**:622-634. DOI: 10.1016/j.joule.2023.12.020

[79] Shi X, Chen H, Hao F, Liu R, Wang T, Qiu P, et al. Room-temperature ductile inorganic semiconductor. Nature Materials. 2018;**17**:421-426. DOI: 10.1038/s41563-018-0047-z

[80] Deng T, Gao Z, Li Z, Qiu P, Li Z, Yuan X, et al. Room-temperature exceptional plasticity in defective $Bi_2Te_3$-based bulk thermoelectric crystals. Science. 2024;**386**:1112-1117. DOI: 10.1126/science.adr8450

[81] Liu C, Lu B, Yan J, Xu J, Yue R, Zhu Z, et al. Highly conducting free-standing poly (3, 4-ethylenedioxythiophene)/poly (styrenesulfonate) films with improved thermoelectric performances. Synthetic Metals. 2010;**160**:2481-2485. DOI: 10.1016/j.synthmet.2010.09.031

[82] Mengistie DA, Chen CH, Boopathi KM, Pranoto FW, Li LJ, Chu CW. Enhanced thermoelectric performance of PEDOT: PSS flexible bulky papers by treatment with secondary dopants. ACS Applied Materials & Interfaces. 2015;**7**:94-100. DOI: 10.1021/am507032e

[83] Ni D, Song H, Chen Y, Cai K. Significantly enhanced thermoelectric performance of flexible PEDOT nanowire film via coating Te

nanostructures. Journal of Materiomics. 2020;**6**:364-370. DOI: 10.1016/j.jmat.2019.07.001

[84] Jia F, Wu R, Liu C, Lan J, Lin YH, Yang X. High thermoelectric and flexible PEDOT/SWCNT/BC nanoporous films derived from aerogels. ACS Sustainable Chemistry & Engineering. 2019;**7**:12591-12600. DOI: 10.1021/acssuschemeng.9b02518

[85] Du Y, Shen SZ, Yang WD, Chen S, Qin Z, Cai KF, et al. Facile preparation and characterization of poly (3-hexylthiophene)/multiwalled carbon nanotube thermoelectric composite films. Journal of Electronic Materials. 2012;**41**:1436-1441. DOI: 10.1007/s11664-012-1931-y

[86] Ni D, Song H, Chen Y, Cai K. Free-standing highly conducting PEDOT films for flexible thermoelectric generator. Energy. 2019;**170**:53-61. DOI: 10.1016/j.energy.2018.12.124

[87] Ni D, Chen Y, Song H, Liu C, Yang X, Cai K. Free-standing and highly conductive PEDOT nanowire films for high-performance all-solid-state supercapacitors. Journal of Materials Chemistry A. 2019;**7**:1323-1333. DOI: 10.1039/C8TA08814D

[88] Wang J, Cai K, Song H, Shen S. Simultaneously enhanced electrical conductivity and seebeck coefficient in Poly (3, 4-ethylenedioxythiophene) films treated with hydroiodic acid. Synthetic Metals. 2016;**220**:585-590. DOI: 10.1016/j.synthmet.2016.07.023

[89] Bubnova O, Khan ZU, Malti A, Braun S, Fahlman M, Berggren M, et al. Optimization of the thermoelectric figure of merit in the conducting polymer poly (3, 4-ethylenedioxythiophene). Nature Materials. 2011;**10**:429-433. DOI: 10.1038/nmat3012

[90] Fan Z, Du D, Guan X, Ouyang J. Polymer films with ultrahigh thermoelectric properties arising from significant seebeck coefficient enhancement by ion accumulation on surface. Nano Energy. 2018;**51**:481-488. DOI: 10.1016/j.nanoen.2018.07.002

[91] Kim N, Kee S, Lee SH, Lee BH, Kahng YH, Jo YR, et al. Highly conductive PEDOT: PSS nanofibrils induced by solution-processed crystallization. Advanced Materials. 2014;**26**:2268-2272. DOI: 10.1002/adma.201304611

[92] Fan Z, Li P, Du D, Ouyang J. Significantly enhanced thermoelectric properties of PEDOT: PSS films through sequential post-treatments with common acids and bases. Advanced Energy Materials. 2017;**7**:1602116. DOI: 10.1002/aenm.201602116

[93] Guan X, Cheng H, Ouyang J. Significant enhancement in the Seebeck coefficient and power factor of thermoelectric polymers by the Soret effect of polyelectrolytes. Journal of Materials Chemistry A. 2018;**6**:19347-19352. DOI: 10.1039/C8TA08387H

[94] Zhang S, Fan Z, Wang X, Zhang Z, Ouyang J. Enhancement of the thermoelectric properties of PEDOT: PSS via one-step treatment with cosolvents or their solutions of organic salts. Journal of Materials Chemistry A. 2018;**6**:7080-7087. DOI: 10.1039/C7TA11148G

[95] Fan Z, Du D, Yu Z, Li P, Xia Y, Ouyang J. Significant enhancement in the thermoelectric properties of PEDOT: PSS films through a treatment with organic solutions of inorganic salts. ACS Applied Materials & Interfaces. 2016;**8**:23204-23211. DOI: 10.1021/acsami.6b07234

[96] Tsai TC, Chang HC, Chen CH, Whang WT. Widely variable Seebeck

coefficient and enhanced thermoelectric power of PEDOT: PSS films by blending thermal decomposable ammonium formate. Organic Electronics. 2011;**12**:2159-2164. DOI: 10.1016/j.orgel.2011.09.004

[97] Zhang L, Goto T, Imae I, Sakurai Y, Harima Y. Thermoelectric properties of PEDOT films prepared by electrochemical polymerization. Journal of Polymer Science Part B: Polymer Physics. 2017;**55**:524-531. DOI: 10.1002/polb.24299

[98] Yi C, Wilhite A, Zhang L, Hu R, Chuang SS, Zheng J, et al. Enhanced thermoelectric properties of poly (3, 4-ethylenedioxythiophene): poly (styrenesulfonate) by binary secondary dopants. ACS Applied Materials & Interfaces. 2015;**2015**(7):8984-8989. DOI: 10.1021/acsami.5b01960

[99] An CJ, Kang YH, Song H, Jeong Y, Cho SY. High-performance flexible thermoelectric generator by control of electronic structure of directly spun carbon nanotube webs with various molecular dopants. Journal of Materials Chemistry A. 2017;**5**:15631-15639. DOI: 10.1039/C7TA02509B

[100] Zhou W, Fan Q, Zhang Q, Cai L, Li K, Gu X, et al. High-performance and compact-designed flexible thermoelectric modules enabled by a reticulate carbon nanotube architecture. Nature Communications. 2017;**8**:14886. DOI: 10.1038/ncomms14886

[101] Du Y, Cai KF, Shen SZ, Casey PS. Preparation and characterization of graphene nanosheets/poly (3-hexylthiophene) thermoelectric composite materials. Synthetic Metals. 2012;**162**:2102-2106. DOI: 10.1016/j.synthmet.2012.09.011

[102] Du Y, Shen SZ, Yang WD, Cai KF, Casey PS. Preparation and characterization of multiwalled carbon nanotube/poly (3-hexylthiophene) thermoelectric composite materials. Synthetic Metals. 2012;**162**:375-380. DOI: 10.1016/j.synthmet.2011.12.023

[103] Wu R, Yuan H, Liu C, Lan JL, Yang X, Lin YH. Flexible PANI/SWCNT thermoelectric films with ultrahigh electrical conductivity. RSC Advances. 2018;**8**:26011-26019. DOI: 10.1039/C8RA04863K

[104] Xu Q, Qu S, Ming C, Qiu P, Yao Q, Zhu C, et al. Conformal organic–inorganic semiconductor composites for flexible thermoelectrics. Energy & Environmental Science. 2020;**13**:511-518. DOI: 10.1039/C9EE03776D

[105] Du Y, Cai KF, Chen S, Cizek P, Lin T. Facile preparation and thermoelectric properties of $Bi_2Te_3$ based alloy nanosheet/PEDOT:PSS composite films. ACS Applied Materials & Interfaces. 2014;**6**:5735-5743. DOI: 10.1021/am5002772

[106] Ju H, Kim J. Chemically exfoliated SnSe nanosheets and their SnSe/poly (3, 4-ethylenedioxythiophene): poly (styrenesulfonate) composite films for polymer based thermoelectric applications. ACS Nano. 2016;**10**:5730-5739. DOI: 10.1021/acsnano.5b07355

[107] Ju H, Park D, Kim J. Solution-processable flexible thermoelectric composite films based on conductive polymer/$SnSe_{0.8}$ $S_{0.2}$ nanosheets/carbon nanotubes for wearable electronic applications. Journal of Materials Chemistry A. 2018;**6**:5627-5634. DOI: 10.1039/C7TA11285H

[108] Li J, Shi Q, Röhr JA, Wu H, Wu B, Guo Y, et al. Flexible 3D porous $MoS_2$/CNTs architectures with ZT of 0.17 at room temperature for wearable thermoelectric applications. Advanced

Functional Materials. 2020;**30**:2002508. DOI: 10.1002/adfm.202002508

[109] Hernandez Y, Nicolosi V, Lotya M, Blighe FM, Sun Z, De S, et al. High-yield production of graphene by liquid-phase exfoliation of graphite. Nature Nanotechnology. 2008;**3**:563-568. DOI: 10.1038/nnano.2008.215

[110] Wang L, Zhang Z, Geng L, Yuan T, Liu Y, Guo J, et al. Solution-printable fullerene/$TiS_2$ organic/inorganic hybrids for high-performance flexible n-type thermoelectrics. Energy & Environmental Science. 2018;**11**:1307-1317. DOI: 10.1039/C7EE03617E

[111] Dun C, Hewitt CA, Huang H, Xu J, Zhou C, Huang W, et al. Flexible n-type thermoelectric films based on Cu-doped $Bi_2Se_3$ nanoplate and polyvinylidene fluoride composite with decoupled Seebeck coefficient and electrical conductivity. Nano Energy. 2015;**18**:306-314

[112] Wan C, Tian R, Kondou M, Yang R, Zong P, Koumoto K. Ultrahigh thermoelectric power factor in flexible hybrid inorganic-organic superlattice. Nature Communications. 2017;**8**:1024. DOI: 10.1038/s41467-017-01149-4

[113] Song H, Qiu Y, Wang Y, Cai K, Li D, Deng Y, et al. Polymer/carbon nanotube composite materials for flexible thermoelectric power generator. Composites Science and Technology. 2017;**153**:71-83. DOI: 10.1016/j.compscitech.2017.10.006

[114] Meng Q, Cai K, Du Y, Chen L. Preparation and thermoelectric properties of SWCNT/PEDOT:PSS coated tellurium nanorod composite films. Journal of Alloys and Compounds. 2018;**778**:163-169. DOI: 10.1016/j.jallcom.2018.10.381

[115] Song H, Cai K. Preparation and properties of PEDOT:PSS/Te nanorod composite films for flexible thermoelectric power generator. Energy. 2017;**125**:519-525. DOI: 10.1016/j.energy.2017.01.037

[116] Fan W, Guo CY, Chen G. Flexible films of poly (3, 4-ethylenedioxythiophene)/carbon nanotube thermoelectric composites prepared by dynamic 3-phase interfacial electropolymerization and subsequent physical mixing. Journal of Materials Chemistry A. 2018;**6**:12275-12280. DOI: 10.1039/C8TA04838J

[117] Zeng X, Yan C, Ren L, Zhang T, Zhou F, Liang X, et al. Silver telluride nanowire assembly for high-performance flexible thermoelectric film and its application in self-powered temperature sensor. Advanced Electronic Materials. 2019;**5**:1800612. DOI: 10.1002/aelm.201800612

[118] Abdullah SM, Ahmad Z, Sulaiman K. A solution-based temperature sensor using the organic compound CuTsPc. Sensors. 2014;**14**:9878-9888. DOI: 10.3390/s140609878

[119] Nichols WW. Clinical measurement of arterial stiffness obtained from noninvasive pressure waveforms. American Journal of Hypertension. 2005;**18**:3S-10S. DOI: 10.1016/j.amjhyper.2004.10.009

[120] Trung TQ, Dang TML, Ramasundaram S, Toi PT, Park SY, Lee NE. A stretchable strain-insensitive temperature sensor based on free-standing elastomeric composite fibers for on-body monitoring of skin temperature. ACS Applied Materials & Interfaces. 2018;**11**:2317-2327. DOI: 10.1021/acsami.8b19425

[121] Huang Y, Zeng X, Wang W, Guo X, Hao C, Pan W, et al. High-resolution flexible temperature sensor based graphite-filled polyethylene oxide and polyvinylidene fluoride composites for body temperature monitoring. Sensors and Actuators A: Physical. 2018;**278**:1-10. DOI: 10.1016/j.sna.2018.05.024

[122] Wang X, Meng F, Wang T, Li C, Tang H, Gao Z, et al. High performance of PEDOT:PSS/SiC-NWs hybrid thermoelectric thin film for energy harvesting. Journal of Alloys and Compounds. 2018;**734**:121-129. DOI: 10.1016/j.jallcom.2017.11.013

[123] See KC, Feser JP, Chen CE, Majumdar A, Urban JJ, Segalman RA. Water-processable polymer–nanocrystal hybrids for thermoelectrics. Nano Letters. 2010;**10**:4664-4667. DOI: 10.1021/nl102880k

[124] Novak TG, Kim J, Kim J, Shin H, Tiwari AP, Song JY, et al. Flexible thermoelectric films with high power factor made of non-oxidized graphene flakes. 2D Materials. 2019;**6**:045019. DOI: 10.1088/2053-1583/ab2c32

[125] Zhu W, Deng Y, Cao L. Light-concentrated solar generator and sensor based on flexible thin-film thermoelectric device. Nano Energy. 2017;**34**:463-471. DOI: 10.1016/j.nanoen.2017.03.020

[126] Singkaselit K, Sakulkalavek A, Sakdanuphab R. Effects of annealing temperature on the structural, mechanical and electrical properties of flexible bismuth telluride thin films prepared by high-pressure RF magnetron sputtering. Advances in Natural Sciences: Nanoscience and Nanotechnology. 2017;**8**:035002. DOI: 10.1088/2043-6254/aa7222

[127] Nuthongkum P, Sakdanuphab R, Horprathum M, Sakulkalavek A. [Bi]:[Te] control, structural and thermoelectric properties of flexible $Bi_xTe_y$ thin films prepared by RF magnetron sputtering at different sputtering pressures. Journal of Electronic Materials. 2017;**46**:6444-6450. DOI: 10.1007/s11664-017-5671-x

[128] Kong D, Zhu W, Guo Z, Deng Y. High-performance flexible $Bi_2Te_3$ films based wearable thermoelectric generator for energy harvesting. Energy. 2019;**175**:292-299. DOI: 10.1016/j.energy.2019.03.060

[129] Shen S, Zhu W, Deng Y, Zhao H, Peng Y, Wang C. Enhancing thermoelectric properties of $Sb_2Te_3$ flexible thin film through microstructure control and crystal preferential orientation engineering. Applied Surface Science. 2017;**414**:197-204. DOI: 10.1016/j.apsusc.2017.04.074

[130] Khumtong T, Sukwisute P, Sakulkalavek A, Sakdanuphab R. Microstructure and electrical properties of antimony telluride thin films deposited by RF magnetron sputtering on flexible substrate using different sputtering pressures. Journal of Electronic Materials. 2017;**46**:3166-3171. DOI: 10.1007/s11664-017-5303-5

[131] Jitthamapirom P, Wanarattikan P, Nuthongkum P, Sakdanuphab R, Sakulkalavek A. Comparison of thermoelectric properties of flexible bismuth telluride thin films deposited via DC and RF magnetron sputtering. Ferroelectrics. 2019;**552**:64-72. DOI: 10.1080/00150193.2019.1653083

[132] Fan P, Zhang PC, Liang GX, Li F, Chen YX, Luo JT, et al. High-performance bismuth telluride thermoelectric thin films fabricated by using the two-step single-source thermal evaporation. Journal of Alloys and Compounds. 2020;**819**:153027. DOI: 10.1016/j.jallcom.2019.153027

[133] Shang H, Li T, Luo D, Yu L, Zou Q, Huang D, et al. High-performance Ag-modified $Bi_{0.5}Sb_{1.5}Te_3$ films for the flexible thermoelectric generator. ACS Applied Materials & Interfaces. 2020;**12**:7358-7365. DOI: 10.1021/acsami.9b21771

[134] Kim BG, Bae SH, Byeon J, Lee C, Choi SM. Stress-induced change of Cu-doped $Bi_2Te_3$ thin films for flexible thermoelectric applications. Materials Letters. 2020;**270**:127697. DOI: 10.1016/j.matlet.2020.127697

[135] Vieira E, Figueira J, Pires AL, Grilo J, Silva MF, Pereira AM, et al. $Bi_2Te_3$ and $Sb_2Te_3$ thin films with enhanced thermoelectric properties for flexible thermal sensors. Proceedings. 2018;**2**:815. DOI: 10.3390/proceedings2130815

[136] Fan P, Fan WF, Zheng ZH, Zhang Y, Luo JT, Liang GX, et al. Thermoelectric properties of zinc antimonide thin film deposited on flexible polyimide substrate by RF magnetron sputtering. Journal of Materials Science: Materials in Electronics. 2014;**25**:5060-5065. DOI: 10.1007/s10854-014-2271-x

[137] Zheng ZH, Li F, Luo JT, Liang GX, Ma HL, Zhang XH, et al. Enhancement of power factor in zinc antimonide thermoelectric thin film doped with titanium. Materials Letters. 2017;**209**:455-458. DOI: 10.1016/j.matlet.2017.08.063

[138] Kusano K, Yamamoto A, Nakata M, Suemasu T, Toko K. Thermoelectric inorganic SiGe film synthesized on flexible plastic substrate. ACS Applied Energy Materials. 2018;**1**:5280-5285. DOI: 10.1021/acsaem.8b00899

[139] Coroa J, Faustino BM, Marques A, Bianchi C, Koskinen T, Juntunen T, et al. Highly transparent copper iodide thin film thermoelectric generator on a flexible substrate. RSC Advances. 2019;**9**:35384-35391. DOI: 10.1039/C9RA07309D

[140] Yang C, Souchay D, Kneiß M, Bogner M, Wei HM, Lorenz M, et al. Transparent flexible thermoelectric material based on non-toxic earth-abundant p-type copper iodide thin film. Nature Communications. 2017;**8**:16076. DOI: 10.1038/ncomms16076

[141] Seo B, Hwang H, Kang S, Cha Y, Choi W. Flexible-detachable dual-output sensors of fluid temperature and dynamics based on structural design of thermoelectric materials. Nano Energy. 2018;**50**:733-743. DOI: 10.1016/j.nanoen.2018.06.027

[142] Umeda K, Uenuma M, Senaha D, Felizco JC, Uraoka Y, Adachi H. Amorphous thin film for thermoelectric application. Journal of Physics: Conference Series. 2018;**1052**:012016

[143] Paul B, Lu J, Eklund P. Nanostructural tailoring to induce flexibility in thermoelectric $Ca_3Co_4O_9$ thin films. ACS Applied Materials & Interfaces. 2017;**9**:25308-25316. DOI: 10.1021/acsami.7b06301

[144] Paul B, Khranovskyy V, Yakimova R, Eklund P. Donor-doped ZnO thin films on mica for fully-inorganic flexible thermoelectrics. Materials Research Letters. 2019;**7**:239-243. DOI: 10.1080/21663831.2019.1594427

[145] Zhong Y, Zhang L, Linseis V, Qin B, Chen W, Zhao LD, et al. High-quality textured SnSe thin films for self-powered, rapid-response photothermoelectric application. Nano Energy. 2020;**2020**(72):104742. DOI: 10.1016/j.nanoen.2020.104742

[146] Cheng H, Du Y, Wang B, Mao Z, Xu H, Zhang L, et al. Flexible

cellulose-based thermoelectric sponge towards wearable pressure sensor and energy harvesting. Chemical Engineering Journal. 2018;**338**:1-7. DOI: 10.1016/j.cej.2017.12.134

[147] Kato K, Hatasako Y, Uchino M, Nakata Y, Suzuki Y, Hayakawa T, et al. Flexible porous bismuth telluride thin films with enhanced figure of merit using micro-phase separation of block copolymer. Advanced Materials Interfaces. 2014;**1**:1300015. DOI: 10.1002/admi.201300015

[148] Rojas JP, Conchouso D, Arevalo A, Singh D, Foulds IG, Hussain MM. Based origami flexible and foldable thermoelectric nanogenerator. Nano Energy. 2017;**31**:296-301

[149] Karttunen AJ, Sarnes L, Townsend R, Mikkonen J, Karppinen M. Flexible thermoelectric ZnO–organic superlattices on cotton textile substrates by ALD/MLD. Advanced Electronic Materials. 2017;**3**:1600459. DOI: 10.1002/aelm.201600459

[150] Kou L, Yan B, Hu F, Wu SC, Wehling TO, Felser C, et al. Graphene-based topological insulator with an intrinsic bulk band gap above room temperature. Nano Letters. 2013;**13**:6251-6255. DOI: 10.1021/nl4037214

[151] Lee CW, Kim GH, Choi JW, An KS, Kim JS, Kim H, et al. Improvement of thermoelectric properties of $Bi_2Te_3$ and $Sb_2Te_3$ films grown on graphene substrate. Physica status solidi (RRL)–Rapid Research Letters. 2017;**11**:1700029. DOI: 10.1002/pssr.201700029

[152] Lee JA, Aliev AE, Bykova JS, Andrade MJ, Kim D, Sim HJ, et al. Woven-yarn thermoelectric textiles. Advanced Materials. 2016;**28**:5038-5044. DOI: 10.1002/adma.201600709

[153] Varghese T, Hollar C, Richardson J, Kempf N, Han C, Gamarachchi P, et al. High-performance and flexible thermoelectric films by screen printing solution-processed nanoplate crystals. Scientific Reports. 2016;**6**:33135. DOI: 10.1038/srep33135

[154] Han C, Tan G, Varghese T, Kanatzidis MG, Zhang Y. High-performance PbTe thermoelectric films by scalable and low-cost printing. ACS Energy Letters. 2018;**3**:818-822. DOI: 10.1021/acsenergylett.8b00041

[155] Danaei R, Varghese T, Ahmadzadeh M, McCloy J, Hollar C, Sadeq Saleh M, et al. Ultrafast fabrication of thermoelectric films by pulsed light sintering of colloidal nanoparticles on flexible and rigid substrates. Advanced Engineering Materials. 2019;**21**:1800800. DOI: 10.1002/adem.201800800

[156] Saeidi-Javash M, Kuang W, Dun C, Zhang Y. 3D conformal printing and photonic sintering of high-performance flexible thermoelectric films using 2D nanoplates. Advanced Functional Materials. 2019;**29**:1901930. DOI: 10.1002/adfm.201901930

[157] Hou W, Nie X, Zhao W, Zhou H, Mu X, Zhu W, et al. Fabrication and excellent performances of $Bi_{0.5}Sb_{1.5}Te_3$/epoxy flexible thermoelectric cooling devices. Nano Energy. 2018;**50**:766-776. DOI: 10.1016/j.nanoen.2018.06.020

[158] Snyder GJ, Lim JR, Huang CK, Fleurial JP. Thermoelectric microdevice fabricated by a MEMS-like electrochemical process. Nature Materials. 2023;**2**:528-531. DOI: 10.1038/nmat943

[159] Goncalves LM, Rocha JG, Couto C, Alpuim P, Min G, Rowe DM, et al. Fabrication of flexible thermoelectric microcoolers using planar thin-film

technologies. Journal of Micromechanics and Microengineering. 2007;**17**:S168. DOI: 10.1088/0960-1317/17/7/S14

[160] Madan D, Wang Z, Chen A, Wright PK, Evans JW. High-performance dispenser printed MA p-type $Bi_{0.5}Sb_{1.5}Te_3$ flexible thermoelectric generators for powering wireless sensor networks. ACS Applied Materials & Interfaces. 2013;**5**:11872-11876. DOI: 10.1021/am403568t

[161] Chen B, Kruse M, Xu B, Tutika R, Zheng W, Bartlett MD, et al. Flexible thermoelectric generators with inkjet-printed bismuth telluride nanowires and liquid metal contacts. Nanoscale. 2019;**11**:5222-5230. DOI: 10.1039/C8NR09101C

[162] Du J, Zhang B, Jiang M, Zhang Q, Zhang K, Liu Y, et al. Inkjet printing flexible thermoelectric devices using metal chalcogenide nanowires. Advanced Functional Materials. 2023;**33**:2213564. DOI: 10.1002/adfm.202213564

[163] Ferhat S, Domain C, Vidal J, Noël D, Ratier B, Lucas B. Flexible thermoelectric device based on $TiS_2(HA)_x$ n-type nanocomposite printed on paper. Organic Electronics. 2019;**68**:256-263. DOI: 10.1016/j.orgel.2019.02.031

[164] Zhao X, Han W, Jiang Y, Zhao C, Ji X, Kong F, et al. A honeycomb-like paper-based thermoelectric generator based on a $Bi_2Te_3$/bacterial cellulose nanofiber coating. Nanoscale. 2019;**11**:17725-17735. DOI: 10.1039/C9NR06197E

[165] Zhao X, Han W, Zhao C, Wang S, Kong F, Ji X, et al. Fabrication of transparent paper-based flexible thermoelectric generator for wearable energy harvester using modified distributor printing technology. ACS Applied Materials & Interfaces. 2019;**11**:10301-10309. DOI: 10.1021/acsami.8b21716

[166] Shin S, Kumar R, Roh JW, Ko DS, Kim HS, Kim S I, et al. High-performance screen-printed thermoelectric films on fabrics. Scientific Reports. 2017;**7**:7317. DOI: 10.1038/s41598-017-07654-2

[167] Hosokawa Y, Wada K, Tanaka M, Tomita K, Takashiri M. Thermal annealing effect on structural and thermoelectric properties of hexagonal $Bi_2Te_3$ nanoplate thin films by drop-casting technique. Japanese Journal of Applied Physics. 2017;**57**:02CC02. DOI: 10.7567/JJAP.57.02CC02

[168] Kimura Y, Mori R, Yonezawa S, Yabuki H, Namiki H, Ota Y, et al. Solvothermal synthesis of n-type $Bi_2(Se_xTe_{1-x})_3$ nanoplates for high-performance thermoelectric thin films on flexible substrates. Scientific Reports. 2020;**10**:6315. DOI: 10.1038/s41598-020-63374-0

[169] Bharti M, Singh A, Samanta S, Debnath AK, Marumoto K, Aswal DK, et al. Elucidating the mechanisms behind thermoelectric power factor enhancement of poly (3, 4-ethylenedioxythiophene): poly (styrenesulfonate) flexible films. Vacuum. 2018;**153**:238-247. DOI: 10.1016/j.vacuum.2018.04.017

[170] Olvera AA, Moroz NA, Sahoo P, Ren P, Bailey TP, Page AA, et al. Partial indium solubility induces chemical stability and colossal thermoelectric figure of merit in $Cu_2Se$. Energy & Environmental Science. 2017;**10**:1668-1676. DOI: 10.1039/C7EE01193H

[171] Lin Z, Hollar C, Kang JS, Yin A, Wang Y, Shiu HY, et al. A solution processable high-performance thermoelectric copper selenide thin film. Advanced Materials. 2017;**29**:1606662. DOI: 10.1002/adma.201606662

[172] Cho C, Wallace KL, Tzeng P, Hsu JH, Yu C, Grunlan JC. Outstanding low temperature thermoelectric power factor from completely organic thin films enabled by multidimensional conjugated nanomaterials. Advanced Energy Materials. 2016;**6**:1502168. DOI: 10.1002/aenm.201502168

[173] Tian R, Wan C, Wang Y, Wei Q, Ishida T, Yamamoto A, et al. A solution-processed $TiS_2$/organic hybrid superlattice film towards flexible thermoelectric devices. Journal of Materials Chemistry A. 2017;**5**:564-570. DOI: 10.1039/C6TA08838D

[174] Choi J, Cho K, Yun J, Park Y, Yang S, Kim S. Large voltage generation of flexible thermoelectric nanocrystal thin films by finger contact. Advanced Energy Materials. 2017;**7**:1700972. DOI: 10.1002/aenm.201700972

[175] Jang E, Poosapati A, Jang N, Hu L, Duffy M, Zupan M, et al. Thermoelectric properties enhancement of p-type composite films using wood-based binder and mechanical pressing. Scientific Reports. 2019;**9**:7869. DOI: 10.1038/s41598-019-44225-z

[176] Tzounis L, Gravalidis C, Vassiliadou S, Logothetidis S. Fiber yarns/CNT hierarchical structures as thermoelectric generators. Materials Today: Proceedings. 2017;**4**:7070-7075. DOI: 10.1016/j.matpr.2017.07.040

[177] Weathers A, Ullah Khan Z, Brooke R, Evans D, Pettes MT, Wenzel Andreasen J, et al. Significant electronic thermal transport in the conducting polymer poly (3, 4-ethylenedioxythiophene). Advanced Materials. 2015;**27**:2101-2106. DOI: 10.1002/adma.201404738

[178] Kim SJ, We JH, Cho BJA. Wearable thermoelectric generator fabricated on a glass fabric. Energy & Environmental Science. 2014;**6**:1959-1965

[179] Chen W, Shi XL, Li M, Liu T, Mao Y, Liu Q, et al. Nanobinders advance screen-printed flexible thermoelectrics. Science. 2024;**6727**:1265-1271. DOI: 10.1126/science.ads5868

[180] King JA, Tucker KW, Vogt BD, Weber EH, Quan C. Electrically and thermally conductive nylon 6, 6. Polymer Composites. 1999;**5**:643-654. DOI: 10.1002/pc.10387

[181] Huang S, Kroschwitz J. Mark Enclyclopedia of Polymer Science and Engineering. Vol. 220. New York, USA: John Wiley & Sons; 1985. p. 244. ISBN:0471887862

[182] Zhang HT, Li SB, White CJB, Ning X, Nie HL, Zhu LM. Studies on electrospun nylon-6/chitosan complex nanofiber interactions. Electrochimica Acta. 2009;**54**:5739-5745. DOI: 10.1016/j.electacta.2009.05.021

[183] Bazbouz MB, Stylios GK. The tensile properties of electrospun nylon 6 single nanofibers. Journal of Polymer Science Part B: Polymer Physics. 2010;**15**:1719-1731. DOI: 10.1002/polb.21993

[184] Ezquerra TA, Canalda JC, Sanz A, Linares A. On the electrical conductivity of PVDF composites with different carbon-based nanoadditives. Colloid and Polymer Science. 2014;**292**:1989-1998. DOI: 10.1007/s00396-014-3252-6

[185] Zhou W, Zuo J, Ren W. Thermal conductivity and dielectric properties of Al/PVDF composites. Composites Part A: Applied Science and Manufacturing. 2012;**4**:658-664. DOI: 10.1016/j.compositesa.2011.11.024

[186] Nasir M, Matsumoto H, Danno T, Minagawa M, Irisawa T, Shioya M, et al.

Control of diameter, morphology, and structure of PVDF nanofiber fabricated by electrospray deposition. Journal of Polymer Science Part B: Polymer Physics. 2006;**44**:779-786. DOI: 10.1002/polb.20737

[187] Linares A, Acosta JL. Tensile and dynamic mechanical behaviour of polymer blends based on PVDF. European Polymer Journal. 1997;**4**:467-473. DOI: 10.1016/S0014-3057(96)00182-6

[188] Nishi Y, Iizuka S, Faudree MC, Oyama R. Electrical conductivity enhancement of PTFE (Teflon) induced by homogeneous low voltage electron beam irradiation (HLEBI). Materials Transactions. 2012;**5**:940-945. DOI: 10.2320/matertrans.M2011273

[189] Ambroski L. H-film--a new high temperature dielectric. Industrial & Engineering Chemistry Product Research and Development. 1963;**2**:189-194. DOI: 10.1021/i360007a005

[190] Wang XQ, Chen DR, Han JC, Du SY. Crystallization behavior of polytetrafluoroethylene (PTFE). Journal of Applied Polymer Science. 2002;**83**:990-996. DOI: 10.1002/app.2279

[191] Arce J, Palacios A, Alvítez-Temoche D, Mendoza-Azpur G, Romero-Tapia P, Mayta-Tovalino F. Tensile strength of novel nonabsorbable PTFE (Teflon®) versus other suture materials: an in vitro study. International Journal of Dentistry. 2019;**1**:7419708. DOI: 10.1155/2019/7419708

[192] Sessler GM, Hahn B, Yoon DY. Electrical conduction in polyimide films. Journal of Applied Physics. 1986;**1**:318-326. DOI: 10.1063/1.337646

[193] Wang T, Wang M, Fu L, Duan Z, Chen Y, Hou X, et al. Enhanced thermal conductivity of polyimide composites with boron nitride nanosheets. Scientific Reports. 2018;**1**:1557. DOI: 10.1038/s41598-018-19945-3

[194] Srinivas S, Caputo FE, Graham M, Gardner S, Davis RM, McGrath JE, et al. Semicrystalline polyimides based on controlled molecular weight phthalimide end-capped 1,3-bis (4-aminophenoxy) benzene and 3, 3, 4, 4-biphenyltetracarboxylic dianhydride: synthesis, crystallization, melting, and thermal stability. Macromolecules. 1997;**30**:1012-1022. DOI: 10.1021/ma9604597

[195] Dong J, Yin C, Zhao X, Li Y, Zhang Q. High strength polyimide fibers with functionalized graphene. Polymer. 2013;**23**:6415-6424. DOI: 10.1016/j.polymer.2013.09.035

[196] Zhang HB, Zheng WG, Yan Q, Yang Y, Wang JW, Lu ZH, et al. Electrically conductive polyethylene terephthalate/graphene nanocomposites prepared by melt compounding. Polymer. 2010;**5**:1191-1196. DOI: 10.1016/j.polymer.2010.01.027

[197] Amborski LE, Flierl DW. Physical properties of polyethylene terephthalate films. Industrial & Engineering Chemistry. 1953;**45**:2290-2295. DOI: 10.1021/ie50526a042

[198] Shaikh FUA. Tensile and flexural behaviour of recycled polyethylene terephthalate (PET) fibre reinforced geopolymer composites. Construction and Building Materials. 2020;**245**:118438. DOI: 10.1016/j.conbuildmat.2020.118438

[199] Calvert P. A Review of: "HANDBOOK OF PLASTICS, ELASTOMERS AND COMPOSITES" Second edition edited by CA Harper McGraw Hill 11 West 19th Street New York, NY10011 960 pages,

hard cover, 1992. Material and Manufacturing Process. 1993;**6**:751-752. DOI: 10.1080/10426919308934880

[200] Cygan PJ, Zheng JP, Yen SP, Jow TR. Thermal treatment of polyethylene-2, 6-naphthalate (PEN) film and its influence on the morphology and dielectric strength. In: Proceedings of the Proceedings of IEEE Conference on Electrical Insulation and Dielectric Phenomena-(CEIDP'93). Arlington, USA: IEEE; 1993. pp. 630-635. DOI: 10.1109/CEIDP.1993.378902

[201] Hine PJ, Astruc A, Ward IM. Hot compaction of polyethylene naphthalate. Journal of Applied Polymer Science. 2004;**2**:796-802. DOI: 10.1002/app.20517

[202] Teoh H, Mac Innes D, Metz PD. Electrical conductivity of doped polyacrylonitrile (PAN). Le Journal de Physique Colloques. 1983;**44**:C3-C687. DOI: 10.1051/jphyscol:19833134

[203] Sabetzadeh N, Bahrambeygi H, Rabbi A, Nasouri K. Thermal conductivity of polyacrylonitrile nanofibre web in various nanofibre diameters and surface densities. IET Micro & Nano Letters. 2012;**7**:662-666. DOI: 10.1049/mnl.2012.0375

[204] Gupta A, Singhal R, Bajaj P, Agarwal V. Effect of copolymerization with methacrylonitrile on the dielectric relaxation of polyacrylonitrile. Journal of Applied Polymer Science. 1983;**28**:1167-1177. DOI: 10.1002/app.1983.070280322

[205] Wu T, Lu C, Sun T, Li Y, Yuan S, Li D, et al. New discovery on the relationship between microstructure and tensile strength of PAN-based carbon fibers. Microporous and Mesoporous Materials. 2022;**330**:111584. DOI: 10.1016/j.micromeso.2021.111584

[206] Saltas V, Pentari D, Vallianatos F. Complex electrical conductivity of biotite and muscovite micas at elevated temperatures: A comparative study. Materials. 2020;**16**:3513. DOI: 10.3390/ma13163513

[207] Zhang Z, Feng Y, Wang D, Liang L, Wang Z, Yang K, et al. Thermal conductive network construction and enhanced thermal conductivity in mica tape composites for large generator insulation. Composites Science and Technology. 2024;**254**:110671. DOI: 10.1016/j.compscitech.2024.110671

[208] Busigin C, Lahtinen R, Martinez GM, Thomas G, Woodhams RT. The properties of mica-filled polypropylenes. Polymer Engineering & Science. 1984;**3**:169-174. DOI: 10.1002/pen.760240303

[209] Abdel-karim AM, Salama AH, Hassan ML. Electrical conductivity and dielectric properties of nanofibrillated cellulose thin films from bagasse. Journal of Physical Organic Chemistry. 2018;**9**:e3851. DOI: 10.1002/poc.3851

[210] Brown R. In: Brandrup J, Immergut EH, editors. Polymer handbook. New York: Wiley Interscience; 1989. ISBN 0-471-81244-7

[211] Nordin SB, Nyren JO, Back EL. An indication of molten cellulose produced in a laser beam. Textile Research Journal. 1974;**44**:152-154. DOI: 10.1177/004051757404400211

[212] Wanigaratne DM, Batchelor WJ, Parker IH. Comparison of fracture toughness of paper with tensile properties. Appita Journal. 2002;**5**:369-374

[213] Júnior CP, De Carvalho LH, Fonseca VM, Monteiro SN, d'Almeida JRM. Analysis of the tensile

strength of polyester/hybrid ramie–cotton fabric composites. Polymer Testing. 2004;**2**:131-135. DOI: 10.1016/S0142-9418(03)00071-0

[214] Ma PC, Tang BZ, Kim JK. Effect of CNT decoration with silver nanoparticles on electrical conductivity of CNT-polymer composites. Carbon. 2008;**11**:1497-1505. DOI: 10.1016/j.carbon.2008.06.048

[215] Fujii M, Zhang X, Xie H, Ago H, Takahashi K, Ikuta T, et al. Measuring the thermal conductivity of a single carbon nanotube. Physical Review Letters. 2005;**6**:065502. DOI: 10.1103/PhysRevLett.95.065502

[216] Zhang K, Stocks GM, Zhong J. Melting and premelting of carbon nanotubes. Nanotechnology. 2007;**18**:285703. DOI: 10.1088/0957-4484/18/28/285704

[217] Bai Y, Zhang R, Ye X, Zhu Z, Xie H, Shen B, et al. Carbon nanotube bundles with tensile strength over 80 GPa. Nature Nanotechnology. 2018;**7**:589-595. DOI: 10.1038/s41565-018-0141-z

[218] Chen H, Müller MB, Gilmore KJ, Wallace GG, Li D. Mechanically strong, electrically conductive, and biocompatible graphene paper. Advanced Materials. 2008;**18**:3557-3561

[219] Ghosh D, Calizo I, Teweldebrhan D, Pokatilov EP, Nika DL, Balandin AA, et al. Extremely high thermal conductivity of graphene: Prospects for thermal management applications in nanoelectronic circuits. Applied Physics Letters. 2008;**92**:151911. DOI: 10.1063/1.2907977

[220] Ganz E, Ganz AB, Yang L, Dornfeld M. The initial stages of melting of graphene between 4000 K and 6000 K. Physical Chemistry Chemical Physics. 2017;**19**:3756-3762. DOI: 10.1039/C6CP06940A

[221] Mazrouaa AM, Mansour NA, Abed MY, Youssif MA, Shenashen MA, Awual MR. Nano-composite multi-wall carbon nanotubes using poly (p-phenylene terephthalamide) for enhanced electric conductivity. Journal of Environmental Chemical Engineering. 2019;**2**:103002. DOI: 10.1016/j.jece.2019.103002

[222] Ventura G, Barucci M, Gottardi E, Peroni I. Low temperature thermal conductivity of Kevlar. Cryogenics. 2000;**40**:489-491. DOI: 10.1016/S0011-2275(00)00062-X

[223] Tanner D, Fitzgerald JA, Phillips BR. The kevlar story-an advanced materials case study. Angewandte Chemie International Edition. 1989;**28**:649-654. DOI: 10.1002/anie.198906491

[224] Lu Z, Si L, Zhao Y, Huang J, Yao C, Jia F, et al. Enhanced mechanical and electrical insulating properties of (poly (para-phenylene terephthamide)) PPTA-based specialty paper with nanoscale PPTA fibers. Journal of Materials Science: Materials in Electronics. 2019;**30**:14414-14423. DOI: 10.1007/s10854-019-01811-1

[225] Chen C, Liu Z, Guo L, Huo B, Sun Q, Liang L, et al. High spatiotemporal resolution biomimetic thermoreceptors realizing by jointless p-n integration thermoelectric composites. Advanced Functional Materials. 2024;**49**:2411490. DOI: 10.1002/adfm.202411490

[226] Li G, Hu Y, Chen J, Liang L, Liu Z, Fu J, et al. Thermoelectric and photoelectric dual modulated sensors for human internet of things application in accurate fire recognition and warning. Advanced Functional Materials.

2023;**41**:2303861. DOI: 10.1002/adfm.202303861

[227] Du C, Cao M, Li G, Hu Y, Zhang Y, Liang L, et al. Toward precision recognition of complex hand motions: wearable thermoelectrics by synergistic 2D nanostructure confinement and controlled reduction. Advanced Functional Materials. 2022;**36**:2206083. DOI: 10.1002/adfm.202206083

[228] Dong G, Feng J, Qiu G, Yang Y, Chen Q, Xiong Y, et al. Oriented $Bi_2Te_3$-based films enabled high performance planar thermoelectric cooling device for hot spot elimination. Nature Communications. 2024;**1**:9695. DOI: 10.1038/s41467-024-54017-3